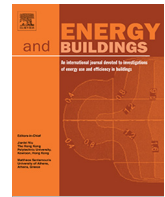




ELSEVIER

Contents lists available at ScienceDirect



Optimization of PV modules layout on high-rise building skins using a BIM-based generative design approach

Faridaddin Vahdatikhaki ^a, Negar Salimzadeh ^b, Amin Hammad ^{c,*}

^a Department of Construction Management and Engineering, University of Twente, the Netherlands

^b Department of Building, Civil, and Environmental Engineering, Concordia University, Montreal, Quebec, Canada

^c Concordia Institute for Information Systems Engineering, Montreal, Quebec, Canada

ARTICLE INFO

Article history:

Received 6 August 2021

Revised 29 November 2021

Accepted 14 December 2021

Available online 18 December 2021

Keywords:

BIM

PV modules

Generative design

Simulation

Optimization

Optimum PV layout

ABSTRACT

Global economic growth is leading to a higher demand for energy. Considering the declining cost of technology and rising fossil fuel prices, the application of renewable energy technologies is promising. The worldwide use of photovoltaic electricity is growing rapidly by more than 50% a year. In the urban environment, buildings are central to human activities. Therefore, to achieve sustainable urban development, buildings are of particular importance for distributed renewable energy generation. Of different types of buildings in the built environment, high-rise buildings are of particular interest because of their high potential for harvesting a considerable amount of photovoltaic (PV) energy on vertical and horizontal surfaces. Nevertheless, this high potential is seldom harnessed mainly because the deployment of PV modules on high-rise buildings involves consideration of a complex interplay between various factors that affect the installation of PV modules (e.g., urban canyons, self-shadowing effect, surface-specific PV modules, etc.). This renders the design of PV modules in high-rise buildings a complex optimization problem, one that requires a generative design approach. In recent years, and with the advent and rising popularity of Building Information Modeling (BIM) concept, the apparatus for the implementation of such a comprehensive generative design approach is becoming increasingly available. However, to the best of authors' knowledge, there are currently no frameworks for the BIM-based generative design of PV modules for high-rise buildings. To this end, the present paper made a novel contribution to the body of knowledge by presenting a BIM-based generative design framework for PV module layout design on the whole exterior of tall buildings. This allows designers to consider the complex interaction between building surface types (e.g., windows, walls, etc.), type of PV module (e.g., opaque, semi-transparent, etc.), the efficiency of different PV modules, and the financial aspect of the PV system (i.e., revenue vs. cost at different study period). The results generated by the elaborate case study demonstrated that the generative design framework is capable of offering more favourable solutions (i.e., either or both of reduced costs and increased energy revenue) compared to baseline scenarios. It is observed that, in the majority of the studied scenarios, the optimum solutions favored a more consistent orientation of the panels (i.e., consistent pan and tilt angles across all the panels).

© 2021 Elsevier B.V. All rights reserved.

1. Introduction

Growing urbanism and the higher level of energy demand in cities make photovoltaic (PV) technology an attractive option to generate energy. With the increasing global demand for energy and environmental concerns, as well as the continuous development of renewable technologies, PV energy is growingly becoming a cost-effective operational energy option. Many of the global leading businesses have sensed this opportunity and started to lever-

age it. For instance, Apple and Amazon have an installed capacity of 393.3 MW, and 329.8 MW, respectively [48]. The worldwide use of PV electricity is increasing by more than 50% a year [8]. Considering the decreasing cost of technology and the rising fossil fuel prices, the application of renewable energy technologies is promising. The application of PV systems in the built environment can reduce the need for electricity grid development and consequently minimize transportation loss [30].

The application of PV modules has been widely explored in the built environment. However, the trend of PV application on building surfaces started by focusing on the rooftops of the buildings due to the simplicity of the process. Nevertheless, despite the

* Corresponding author.

E-mail address: Amin.hammad@concordia.ca (A. Hammad).

lower radiation values on the vertical surfaces and the shadow effects of the surrounding objects, vertical surfaces (i.e., facades), especially of high-rise buildings, offer a great potential for the application of PV systems. Facades have fewer structural obstructions in comparison to rooftops such as chimneys, ventilation systems, and antennas. Furthermore, the rate of snow accumulation on facade PV modules is lower.

This high potential is seldom harnessed mainly because the deployment of PV modules on high-rise buildings involves the consideration of a complex interplay between various factors that affect the installation of PV modules [28]. Examples of these factors include climatic and geography related factors, building geometry and the build environment specifications, PV modules and hardware specifications, investment factors, etc. [43]. Therefore, a successful design and implementation of PV modules on the facade of high-rise buildings need to be carried out in view of all these influential factors. When the economic aspect of deploying solar energy is added to the mentioned technical aspects, the PV modules design becomes a complex multi-objective optimization problem that requires a robust framework. In other words, a generative design methodology is needed to capture the complexities of PV module design for high-rise buildings.

In recent years, Building Information Modeling (BIM) has become an essential part of the design, architecture, and construction process. It provides all sorts of building data in an accessible 3D digital representation in advance of construction [55]. With the advent and rising popularity of the BIM concept, the apparatus for the implementation of such a comprehensive generative design approach is becoming increasingly available. Given that BIM models provide a rich repository of geometric and non-geometric data about the lifecycle of buildings, it has been successfully leveraged to solve complex building design optimization problems in the past [39]. However, to the best of authors knowledge, BIM has never been used for the application of generative design concepts to the design of PV systems on high-rise buildings. This is a major limitation in this domain because in the absence of semantically rich BIM models, the majority of approaches for PV system optimization resort to the indiscriminate treatment of building surfaces. This is an oversight because different types of surfaces on the building facade require different types of PV modules to maintain the economic edge of the design.

The authors have previously proposed a BIM-based surface-specific parametric modeling method for the detailed solar simulation on the building using its surface properties [47]. Different factors, such as the location of PV modules on the building surfaces, size, and tilt, and pan angles were considered in the simulation of the solar radiation. However, given the sheer size of the design space for this problem, a parametric model alone is not sufficient because all possible design alternatives cannot be fully explored to find the global optimum. Therefore, it is imperative to integrate an optimization approach with the BIM-based parametric model and establish a full generative design platform.

Generative design was defined for the first time in the 1870s as "devices capable of generating potential solutions to a given problem". Later, the generative design was described as automating the creation of a large number of designs using the user-defined criteria and constraints [10]. The generative design approach was used in different research domains in recent years. For example, a BIM-based rule language is developed by Sydora & Stroulia [55] to automate the generation of interior design models. In a study by Zhang et al. [60], a parametric generative algorithm is developed to design buildings with respect to the energy conservation perspectives, which can improve the energy efficiency of the building in the early design phase and optimize the cost.

This paper aims to develop a BIM-based generative design framework for the design of PV modules layout on high-rise build-

ing skins. In this framework, the surface-specific parametric model of PV modules is integrated with an optimization method to find the optimum design of PV modules layout considering study period, profit margin, harvested PV energy, and cost. This framework will enable designers and investors to apply the generative design paradigm to the use of PV modules on building skin. A case study is developed to investigate the feasibility of the proposed method.

The remainder of the paper is structured as follows. First, a background study is presented. This is then followed by the presentation of the proposed method. Next, the implementation and case study are presented. Finally, the discussions and conclusions are presented.

2. Literature review

2.1. Components of PV modules and cost breakdown

Multiple factors can affect the amount of generated electricity by PV modules. Some of these factors, such as the size, position, number, and efficiency of the utilized PV modules, are design variables. However, some other factors, such as daylight hours and weather condition, are location-specific and therefore not controllable.

In PV system terminology, all components of a PV system other than the modules, such as the inverters, electrical and structural components, etc., are called the Balance of System (BOS). These components contribute to how the system functions. The total cost of a PV system can be categorized into two major parts, including the hardware costs (i.e., PV modules and the BOS) and the soft costs, such as the labor costs, permits, and customer acquisition costs [27]. According to a price breakdown of the PV system, almost 13% of the total price of a PV system belongs to the modules, and the remaining covers the BOS and the soft costs [24]. A standard PV module has an input rate of around 1000 W/m². However, the available modules have 15–20% efficiency at best [56]. As shown in Fig. 1, the estimated cost of a PV module including all fees is \$2.8 per Watt [53].

According to [24], the cost of PV systems has had a significant reduction of up to 60% since 2009. In addition to the utility rate, higher tax credits and incentive programs can significantly improve the financial feasibility of the PV systems. Concerning the significance of the economic aspects in prospering sustainable energy development, some studies explored the application of PV systems from cost-benefit perspectives. For example, in a techno-economic analysis, the life cycle cost (LCC) of the PV modules is combined with a method for visualizing economic performances of the application of PV modules on building envelopes [37]. Considering the installation, and maintenance cost, the investment payback period is calculated as an economic indicator in pixel units in an empirical study. However, most of the critical but controllable design variables, which are essential in the efficiency of a Building-Integrated PV (BIPV) system, are not included in this study.

Few studies compared the cost of BIPV systems with the cost of standard PV modules. For example, James et al. [32] estimated the installed cost of c-Si BIPV at US\$5.02/W vs. US\$5.71/W for a standard c-Si PV module in the case of residential applications. This reduction is explained by the elimination of the cost of the racking system, which offsets the higher cost of the BIPV modules. Verberne and van den Donker [57] found that the cost of BIPV on the pitched roof of a house in the Netherlands is 7–10% more expensive than a standard PV system. More recent studies [16,25,14] found the same trend in general. However, there is no detailed studies about the cost analysis of BIPV on the facades of high-rise buildings.

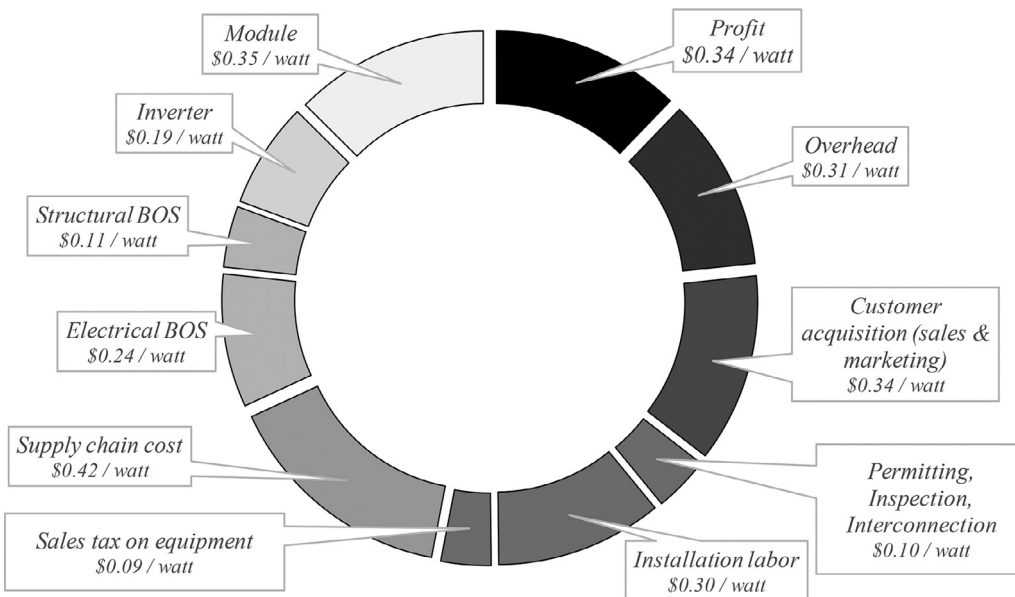


Fig. 1. Cost of PV system breakdown (adapted from [53]).

The absence of an approach that can consider the building surface PV suitability with the optimum PV modules' configurations simultaneously, as well as the economic aspect, necessitates the adoption of an integrated platform that considers all these key factors for designing a financially feasible PV system with the maximum PV energy generation level.

2.2. PV system modeling and optimization approaches on building surfaces

Modeling and optimizing the PV system on building surfaces are among the main challenges of the application of PV in municipalities. In this domain, many researchers considered PV for rooftop surfaces in the built environment. Some merely focused on the 3D modeling [33,7] or solar radiation simulation aspects [20,42]. In some other studies, the optimization of the PV system yield is dis-

cussed just from hardware and technical configuration aspects [11].

As shown in Table 1, several optimization approaches were proposed for rooftop PV layout. However, the majority of them did not use the BIM model in the optimization process. For example, in a study by Cheng et al. [12] to find out the optimal PV angle, 20 south-oriented tilted rooftops are selected and the correlation between the performance of the PV system and the tilt angle are studied. The results revealed that the optimum performance of the roof-mounted PV system is achieved when the tilt angle is equal to the site latitude.

An integrated Geographic Information System (GIS), optimization, and simulation framework is developed by Kucuksari et al. [35] to determine the optimal PV size and location on the Arizona University campus. In this study, the best candidate rooftops with higher radiation potential are simply identified using [2] and the Digital Elevation Model (DEM). Then, considering the area of these

Table 1

Various PV system optimization approaches on building surfaces.

Reference	Sensitivity Analysis	Optimization				Decision Variables	Approach	Modeling Tools			
		Target surfaces	Objective(s)								
			Roof	Facade							
[12]	✓	✓	✓	-	Max PV energy generation	-	✓	✓	-		
[29]	✓	-	✓	-	-	F	V	V	BIM-based		
[35]	-	✓	✓	-	Max total profit of PV installation	-	-	-	GIS-based		
[28]	✓	✓	✓	-	Max annual PV energy generation	-	V	-	GIS-based		
[23]	-	✓	✓	✓	Max PV energy generation, Min system cost	-	F	F	GIS-based		
[34]	-	✓	✓	-	Max PV energy generation, Min initial cost	V	V	-	GIS-based		
[43]	-	✓	✓	-	Min capital investment per unit power output	V	-	V	BIM-based		
[44]	✓	✓	✓	✓	Max PV energy generation, Min cost	-	-	-	Revit		
[1]	-	✓	✓	-	Max PV energy generation	-	-	V	BIM-based		
Present study	✓	✓	✓	✓	Max PV energy generation, Min cost	-	V	V	Dynamo, Refinery		

F: Fixed for all panels, V: Variable per panel.

candidate locations, the maximum number of panels is calculated based on a certain PV panel size. Finally, an optimization module is used to maximize the total profit of the PV deployment, considering the installation, operation, and maintenance costs within a 20-year time horizon. However, in this study, no BIM model is considered and the rooftop analysis is simply based on the DEM model. In addition, the PV location is presented as the only decision variable in the optimization process. GIS-based DEM is a 2.5D model that is simply generated using building's footprint 2D vector maps and the elevation information. The DEM model treats the building skin as a set of polygons and does not provide any surface-specific and semantic information. Therefore, a detailed surface-specific PV layout optimization is not feasible without discriminating between different types of surfaces and their geometrical information.

In another example, a GIS-based optimization model is developed to find out the maximum annual PV energy generation on rooftops after performing a sensitivity analysis considering the azimuth and the tilt angle of the installed panels simultaneously [28].

An integrated multi-objective optimization model was developed by Koo et al. [34] to find the best scenario for implementing the rooftop PV system. However, no BIM model is used in this study, and the analysis was done based on a GIS model.

As shown in Table 1, some of the studies used a BIM-based approach for the rooftop PV optimization but in most of the cases, only a few factors were considered as variables in the optimization process. A BIM-based design and analysis platform for the BIPV on the building surfaces was developed by Ning et al. [44]. The results of the radiation and power flow analysis for a BIPV case study showed that by the implementation of a BIM-based BIPV design, the cost of the PV system was reduced by 11.7% and the power transmission loss decreased by 2.95%. Although this platform is also used for optimization, the focus was only on optimizing the PV array of the rooftop surface.

In addition to the forms and locations of the building exteriors, the shadow of the surrounding objects would highly influence the output of PV modules. For this matter, a tool is developed by Ning et al. [43] to improve the design efficiency of the rooftop PV analysis by performing the shadow and radiation simulation based on the BIM model.

In a study by Al-Janahi et al. [1] the BIM platform was used for the integration of BIPV modules on the rooftop of a metro station with a complex shape in Qatar. First, the rooftop area was divided into 45 main parts, then a certain number of PV modules were considered for each part. The solar feasibility analysis was conducted based on the average annual solar irradiance using Revit. The Genetic Algorithm (GA) was used to optimize the layout of the PV arrays in terms of their electrical connection between those 45 zones in a way to maximize the currents in the rows by reducing the mismatch losses in the strings due to the partial shading. GA, which is inspired by the theory of natural evolution, is one of the well-known *meta-heuristic* methods that can solve complex multi-objective optimization problems [41]. However, in this study, the PV modules with a certain size were directly integrated with the rooftop surfaces and no variation of tilt and pan angles were considered in the process of PV layout optimization.

Lin et al. [38] mentioned the absence of an integrated framework for the design of PV systems, including building modeling and PV simulation. They developed a BIM-based solar tool, which is called PV Link, to integrate the PV system design phases considering various design variables and the feasibility analysis for rooftops. Although the PV placement based on the solar radiation potential on the rooftop is automated in this tool, the optimization approach is still missing in this integrated platform.

Considering the significant amount of potential solar power that could be harvested from high-rise building surfaces, many

studies focused on the application of PV modules on the vertical surfaces of the buildings. However, the application of PV on facade is a complex problem.

Some of the researchers that considered facade PV application, investigated the performance of PV system based on the comparison of various influential factors such as the shadow effect, PV module type, orientation, and architectural aesthetic values. For example, a study by [61], combined aesthetic criteria of BIPV installation with consideration of issues related to functionality, cost, and technical aspects of the applied PV modules.

In a practical application of BIPV on the front facade windows of a building, the impact of the orientation and shadow effect on the performance of the transparent thin film is monitored by Yoon et al. [59]. The analysis of results confirmed that the shadow effect and the orientation of the PV modules can result in 47% improvement in PV systems' performance. However, no optimization is done to find out the optimum trade-off between these factors. In another study, two identical PV systems are applied on two different facades of a building in Turkey with different shading conditions. Comparison of the output for two systems confirmed the criticality of the shading effect on the performance of PV modules [18].

The application of two types of PV modules on a commercial building facade with different tilt angles was simulated and compared by Bueno et al. [9]. Although no cost analysis is conducted in this study, the feasibility of the approach from a financial perspective is found to be viable considering the falling PV system prices.

To assess the PV system performance on the facades of two office buildings, an extensive sensitivity analysis is done by Hwang et al. [29]. The sensitivity analysis result showed that with a certain configuration of the PV modules, 1–5% of the electricity need of an office building can be covered by the installed PV system. Although the impact of multiple factors (e.g. type of the PV module, PV tilt, and orientation) are investigated in PV energy generation, no optimization is done to determine the best combination of the multiple parameters, and no cost analysis is considered within the process.

In a study done by a research group at Lisbon University, extensive work has been done to study the PV potential on building facades [23]. In this study, two reliable simulation approaches are used to prove the feasibility of the facade PV application. As shown in Fig. 2, to find out the best facade PV design that maximizes the total irradiation yield, six irregular facade layouts were modeled in horizontal and vertical forms of rotating or folded louvers in addition to ellipsoid and hexagonal wall geometrical shapes. The Rhinoceros 3D software and Grasshopper were used for parametric modeling of facade PV layout and annual solar radiation analysis with a 0.1 m² grid resolution. The generated energy is calculated by multiplying the total amount of annual solar radiation received by each facade by an average solar cell efficiency of 15%. The results indicated that the horizontal rotated PV layouts on the facade contribute to a higher level of PV energy generation. A multi-objective GA optimization approach is developed to find out the optimum tiling for PV modules string, which leads to maximizing the annual PV energy yield and minimizing the system cost. The optimization results revealed that the layouts with more but shorter PV strings achieve higher energy yields. The operation costs and the discount rate were not considered in the cost calculation. Furthermore, the BIM model was not considered in the analyses and the simulation process was performed based on the Digital Surface Model (DSM) [22].

Considering the PV locations and angles (i.e. tilt and pan) simultaneously on the building surfaces are critical especially when the target buildings are located in a complex built environment such as the dense urban areas where many factors (e.g. interference of shadow caused by the surrounding environment, lower yield con-

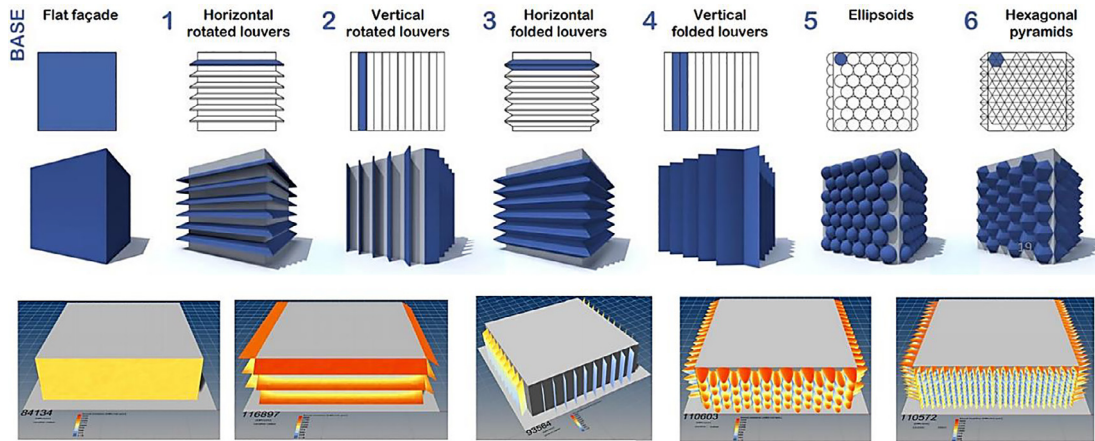


Fig. 2. Studied facade layouts and their respective radiation simulations [22].

tributed by solar radiation angle) affect the performance of the PV system. Therefore, these parameters need to be considered concurrently to find out where and how to apply or integrate the PV modules on the building surfaces to achieve optimum performance.

The limitation of the absence of an integrated PV system simulation and optimization can be resolved using a generative design approach. In the computational design process, the designer develops the procedure that automatically creates a large number of designs. Generative design is a specific application of the computational design approach, which enables the designer to define a set of goals for achieving a design. In this collaborative process between designers and computers, a large number of design alternatives are generated based on the parameters (i.e., decision variables) defined by the designer. Then the computer finds a set of optimal solutions that satisfy the design objectives [50]. Therefore, the process of iterating through options is done by the computer. In addition to providing more chances for designers to focus on creativity, this will accelerate the design process and facilitate the modifications and revision steps [4–6].

The integration of 3D modeling platforms and BIPV simulation tools is proposed in a study by de Sousa Freitas et al. [15] to investigate the feasibility of rooftop and facade BIPV by comparing several design alternatives to retrofit some institutional buildings from the architectural and energy perspective. The design steps, including building 3D modeling, solar radiation assessment, and PV energy generation calculation, are performed using Rhinoceros Grasshopper software [45] and Ladybug [36]. Then, the energy balance is calculated using the BIPV generated energy and the building energy demand. Three design alternatives for facades are proposed as tilted sun-shading elements and double skin facades. Also, three design alternatives with certain tilt and pan angles are proposed for the rooftops along with their energy generation. However, no optimization is considered in the process of modeling and assessment.

As highlighted in Table 1, most of the existing studies focused on PV optimization for rooftop surfaces, and various approaches were proposed by considering different decision variables. However, the majority of them did not use BIM models as the basis,

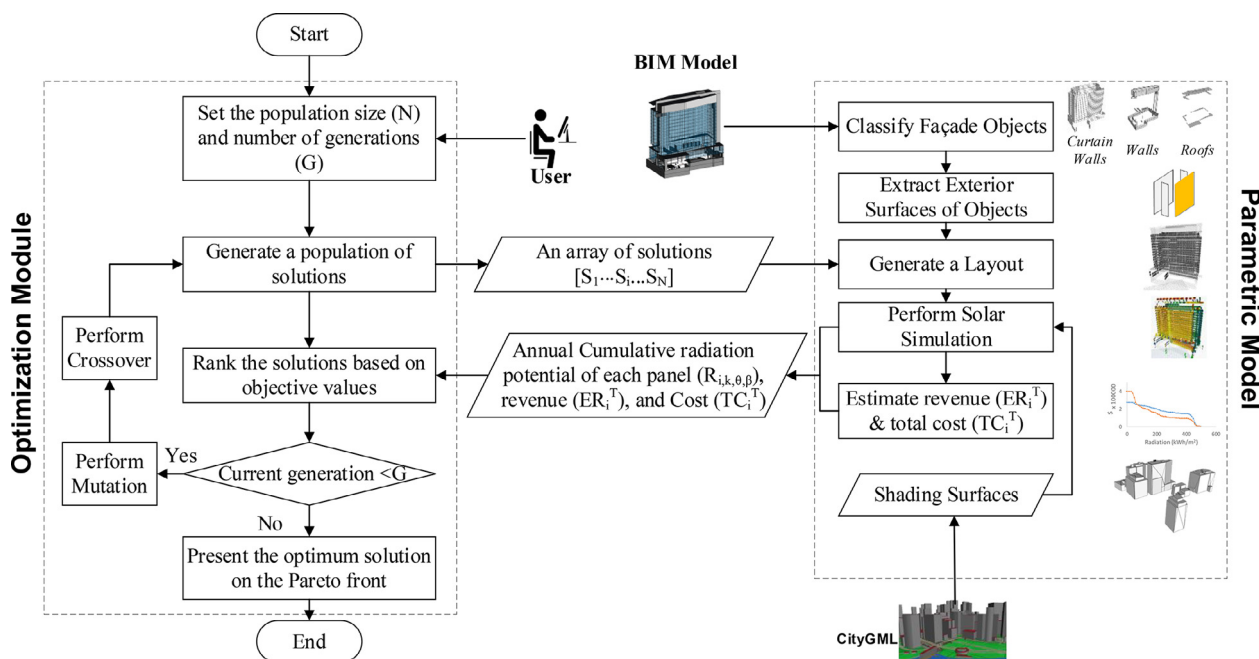


Fig. 3. Overview of the proposed method.

and therefore do not consider surface-suitability for different types of PV modules. Although some studies included the facade surfaces for the application of PV modules, a comprehensive optimization approach based on a surface-specific model, which considers multiple decision variables to optimize the energy yield, cost, and profit, is not developed yet.

3. Proposed framework

Fig. 3 presents the overview of the proposed generative design framework. In this framework, a simulation-based generative design approach is used to find the optimum configurations of PV module layout on the building surfaces considering the revenue of the generated energy and the total life cycle cost. As shown in **Fig. 3**, the proposed framework consists of two main components, namely GA optimization module, and parametric simulation model. In a nutshell, the optimization module generates the initial population of size N . Each member of the population, which represents a specific solution S , is then fed into the simulation model as

the input. The parametric simulation model is then used as a means to assess the objective functions (i.e., revenue and cost). Subsequently, the evolution mechanism of NSGA-II (i.e., the selection, crossover, and mutation) is applied to the results coming from the parametric model. This process is iterated by G generations to identify the optimum solutions, which is represented as a Pareto front.

The overall structure of the proposed parametric model is explained in the previous work of the authors [47]. However, in the interest of completeness, a summary of this model is explained in the following section.

3.1. Parametric model

Fig. 4 presents the overall concept behind the parametric model used in this research. The overall problem of finding the optimum configurations for the PV modules can be translated to (1) identifying the locations where solar panels need to be installed, and (2) finding the tilt and pan angles of these panels (the pan angle is

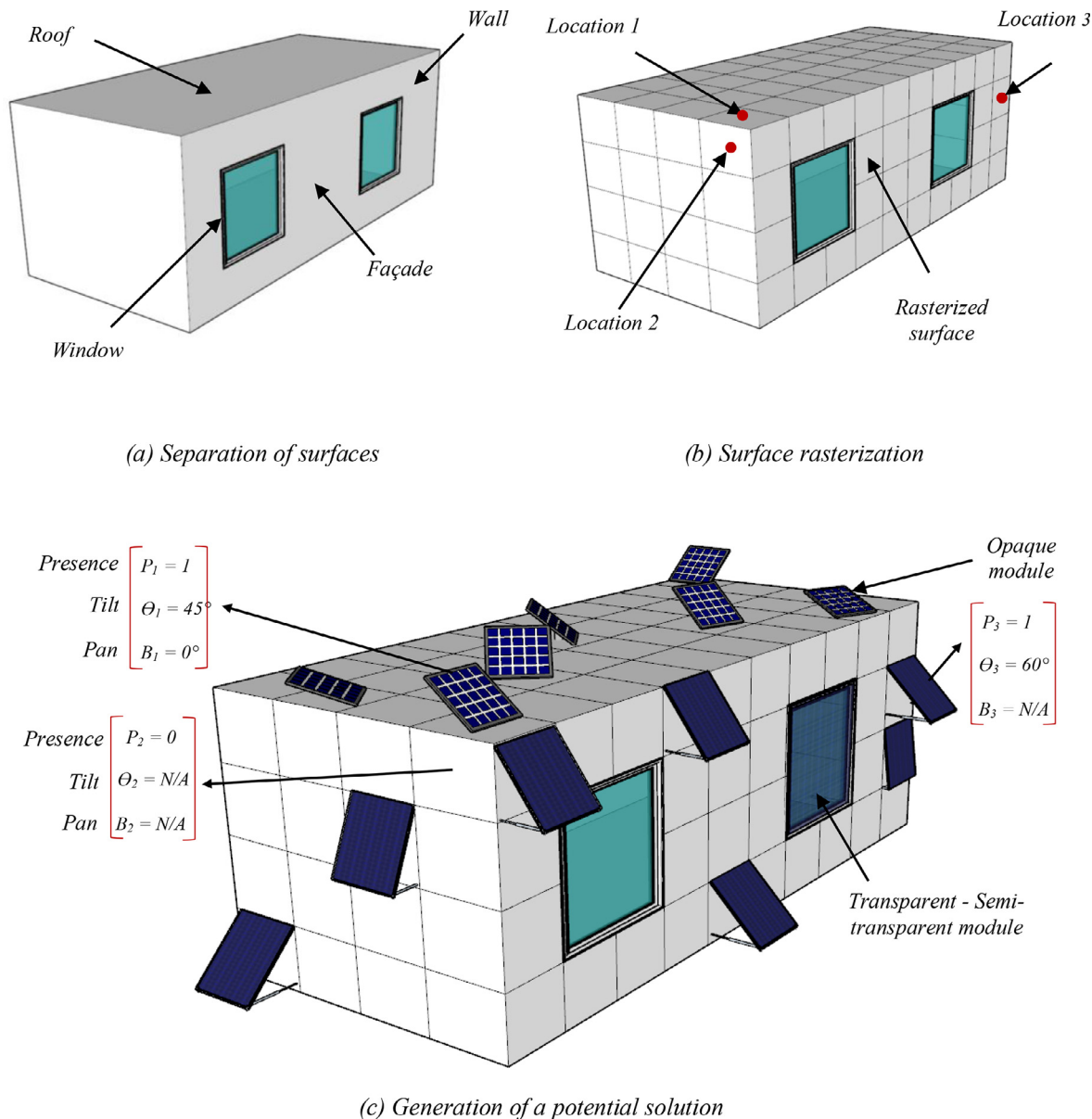


Fig. 4. Process of preparing the model for optimization.

applied only for PV modules on the roof). It should be highlighted that this problem must be solved concurrently for the various variables (i.e., finding optimum locations, pans, and tilts together) rather than sequentially (i.e., to first find the optimum locations and then optimum pans and tilts). This is important because considering the shadow effect of panels on one another, placing PV modules with specific angles on the lower-radiation locations but with a low shadow effect can possibly yield better results than simply placing PV modules on the top-ranking locations from the radiation potential perspective but with a high shadow effect.

The first step in developing viable solutions is to identify all candidate locations considering the suitability of different types of PV modules (e.g., opaque or transparent) on different types of exterior objects (roofs, walls, etc.). Therefore, this research proposes the use of a BIM model as input because the embedded semantics in the BIM model allows considering object-specific PV modules [47]. For example, the use of transparent or semi-transparent panels can be considered only for windows while opaque panels can be considered for the walls (Fig. 4(a)). Additionally, the semantics in the BIM model allows excluding areas where PV modules cannot be installed (e.g., because of mechanical installations or openings).

Once the candidate exterior objects are identified, they can be trimmed to only retain the exterior surface. This is needed because the solar radiation simulation is essentially surface-based. Keeping other surfaces of objects in the model, thus, slows down the simulation considerably. After filtering the redundant surfaces, the remaining surfaces need to be rasterized into a grid, as shown in Fig. 4(b). The size of this grid is determined by the size of the panels being considered for each specific surface. Each cell in this grid is a potential location for the installation of PV modules. Ultimately, the entire exterior of the building is represented by K potential locations for PV modules.

Upon the generation of the simulation grid, a potential solution can be developed. At this stage, the decisions to be made are: (1) should a panel be placed at any of the K locations?, (2) what is the tilt angle of each panel?, and (3) if the panel is on the horizontal surface, what is the pan angle?, as shown in Fig. 4(c). It should be highlighted that the pan angle for the facade PV modules is not considered mainly because of aesthetics reasons and installation challenges. As mentioned by Attoye et al. [3], in some cases aesthetical consideration or other design objectives (e.g., maximum daylight and view) requires compromising the energy performance. The decision about the consideration or rejection of cell k for the installation of PV modules can be mathematically represented by a binary value for P_i , where 0 represents no PV module and 1 represents the use of a PV module on location i . Eventually, a specific solution for PV module installation can be represented by the matrix shown in Eq. (1).

$$S_i = \begin{bmatrix} P_{i,1} & \dots & P_{i,k} & \dots & P_{i,K} \\ \theta_{i,1} & \dots & \theta_{i,k} & \dots & \theta_{i,K} \\ \beta_{i,1} & \dots & \beta_{i,k} & \dots & \beta_{i,K} \end{bmatrix} \quad (1)$$

Where:

S_i : Potential solution i
 $P_{i,k}$: a binary value representing presence (1) or absence (0) of PV module at location k in solution i
 $\theta_{i,k}$: the tilt angle of PV module at location k in solution i where $0^\circ \leq \theta_{i,k} \leq 90^\circ$
 $\beta_{i,k}$: the pan angle of PV module at location k in solution i where $0^\circ \leq \beta_{i,k} \leq 360^\circ$

It should be noted that before the solar radiation simulation can be executed on the generated solution, the simulation engine requires a 3D representation of the surrounding buildings for consideration of their shadow effect on the PV modules. This model can be obtained from available CityGML models or generated using public GIS data. This process is explained in detail in the previous

work of the authors [47]. When the 3D models of the surrounding buildings are imported, the solar radiation simulation can run. This simulation estimates the annual cumulative radiation potential of each panel ($R_{b,k,\theta,\beta}$). This value can then be translated to the required objective values, as will be explained in the next section.

After the calculation of the solar radiation, revenue and cost of each solution is assessed inside the parametric model module. The present value of the energy generated by PV modules during their life cycle of T years for the solution i (ER_i^T) is estimated as shown in Eq. (2).

$$ER_i^T = V \times D_T \sum_{k=1}^K P_{i,k} \times R_{ik\theta\beta} \times e_{i,k} \times PR \quad (2)$$

Where:
 V : the present value of the energy unit cost (\$/kWh)
 D_T : the present value of a growing annuity for T years
 K : the number of possible locations of PV modules
 $P_{i,k}$: a binary value representing presence (1) or absence (0) of PV module at location k in solution i
 $R_{ik\theta\beta}$: the global annual radiation received by PV module k with tilt (θ), and pan (β , only for roof) for solution i (kWh)
 $e_{i,k}$: efficiency of PV module k for the solution i (%)
 PR : the performance ratio of the PV system (%)
 D_T can be calculated using the equation for the present value of a growing annuity as shown in Eq. (3) (Finance [21]), which calculates the present value of a series of future periodic payments that increase at a proportionate rate (i.e., inflation rate).

$$D_T = \frac{1}{r-g} \left[1 - \left(\frac{1+g}{1+r} \right)^T \right] \quad (3)$$

Where r : the discount rate
 g : the inflation rate

The total life cycle cost of PV modules after T years for the solution i (TC_i^T) is calculated as shown in Eq. (4). The total life cycle cost of PV modules includes the initial cost (i.e., acquisition and installation) and the maintenance cost. Since the maintenance cost should be considered for the whole life cycle of the PV system, the D_T factor must be considered.

$$TC_i^T = CM \sum_{k=1}^K a_{i,k} (1 + \alpha \times D_T) \quad (4)$$

Where:
 CM : the cost of PV module per square meter (\$/m²)
 $a_{i,k}$: the area of module k for the solution i (m²)
 α : the percentage of the initial cost of the PV system spent on annual maintenance and operation

3.2. Optimization module

The proposed framework uses Non-Dominated Sorting Genetic Algorithm (NSGA-II) to solve the optimization problem. NSGA-II, which has the ability to effectively solve multi-objective optimization problems, is known as a mature multi-objective optimization algorithm [58]. The algorithm aims to find the optimum location, and tilt and pan angles for the PV modules on the building surfaces given predefined sizes and other attributes of panels. The objective of this optimization is to maximize the revenue (i.e., the monetary value of the generated energy) while minimizing the total life cycle cost (i.e., installation and maintenance).

In the first step of the optimization, the user needs to determine the population size (N) and maximum number of generations (G). In each generation of the solution, NSGA-II generates N number of potential solutions using the chromosome structure shown in Fig. 5. This structure essentially generates a representation of a solution known to the parametric model (i.e., Eq. (1)).

Each chromosome is then sent to the parametric model where the solar simulation is applied and the annual cumulative solar radiation ($R_{b,k,\theta,\beta}$), revenue (ER_i^T), and cost (TC_i^T) of each solution

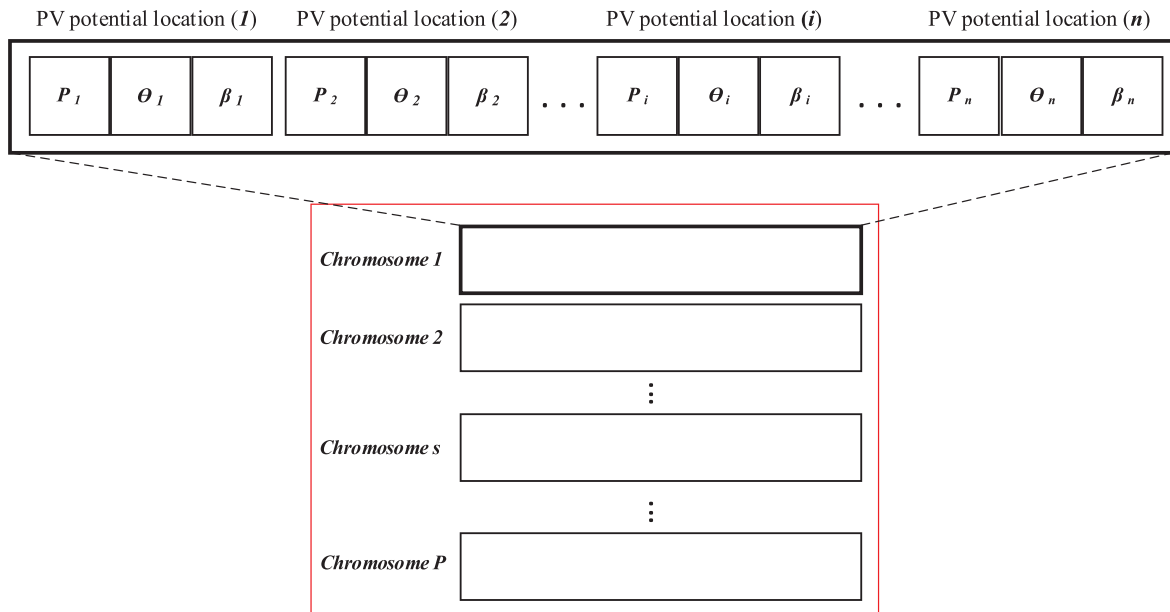


Fig. 5. Example of the GA genes representing the PV potential locations and angles.

in the generation (i.e., each chromosome) is assessed and returned to the optimization module.

Upon receiving the values of the two objective functions, i.e., $\text{Max}(ER_i^T)$ and $\text{Min}(TC_i^T)$, the evolution mechanism of NSGA-II first filters the top-ranking solutions in the generation and then performs mutation and crossover on them to generate the next generation of the solutions. This process is iterated until the solutions reach a predefined level of convergence or the specified number of generations is reached. In the end, the optimum solutions are presented on a Pareto front. This can be used by the user to identify the non-dominant solutions that can be considered for the design of PV modules. Depending on the available budget, the user can determine the preferred solution.

In case the budgetary constraint is not a dominant factor the optimization problem can be solved as a single objective problem by maximizing the profit of the project, which can be calculated as the difference between the revenue (ER_i^T) and total cost (TC_i^T) of each solution. In this case, the final outcome of the optimization is a single solution that generates the maximum profit over T years.

4. Implementation and case study

4.1. Implementation

As shown in Fig. 6, Revit [6] is used as the BIM authoring platform to model the target building. The neighboring buildings were imported into Revit as a CityGML model. To parametrize the generation of specific PV modules on this building, Dynamo [17] is used. Dynamo is a visual programming platform that allows the development of customized scripts and nodes for computational and parametric models. Dynamo runs within Revit and works as an Application Programming Interface (API). Some packages such as Solar Analysis [51] and LunchBox [40] are used in the development process.

The Project Refinery [5] is used as the optimization module in Fig. 3. The seamless integration of Dynamo and Refinery allows us to get the benefits of automating the design option creation process in Refinery, running the custom nodes in Dynamo, and optimizing the solutions in Refinery.

In line with the framework shown in Fig. 3, Refinery generates a generation of solutions. These solutions are fed into Dynamo. It should be highlighted that solar radiation simulation and cost estimation are embedded inside the same parametric model that generates the specific PV layout. So, once the inputs for the layout of the PV system are passed on to the Dynamo model, the Dynamo model creates the layout and performs both the solar radiation simulation and cost estimation. The solar radiation and cost calculations are then returned to Refinery. The selection, crossover, and mutation are applied to the top-ranking solutions in each generation. This process is repeated until the maximum number of generations is reached.

4.2. Case study

The building of John Molson School of Business (JMSB) of Concordia University in downtown Montreal is selected as a case study. This building is selected for the analysis because of its specific architecture, which includes curtain walls, windows, walls, rooftops, and projected horizontal surfaces at a different level (Fig. 7). This complex architecture requires a detailed and surface-specific simulation of the building skin. As explained in Section 4.1, the BIM model of the JMSB building is created using Revit software. To consider the shadow effect of the surrounding buildings in the solar simulation, the city blocks around the JMSB building are extracted from the CityGML model [13]. Then these two models are integrated within Revit. The South-West, North-West, and South-East facades and the rooftop surfaces are selected for the optimization process as shown in Fig. 7(a). This is because the observations from the previous work of the authors [47] suggest that the North-east façade of the building is constantly receiving very low radiation due to the shadow effects of the neighboring buildings as shown in Fig. 7(b) and 7(c). Therefore, the North-East facade of the building is excluded from the generative design.

To calculate the energy generation of the PV system, a performance ratio of $PR = 75\%$ is considered to account for losses induced by inverters, temperature, DC and AC cables, weak radiation, dust, snow, etc. [49]. The average efficiency of $e_{i,k} = 18\%$ is considered [54]. To calculate the present value of a growing annuity D_T of the generated energy, the discount rate and the inflation rate are

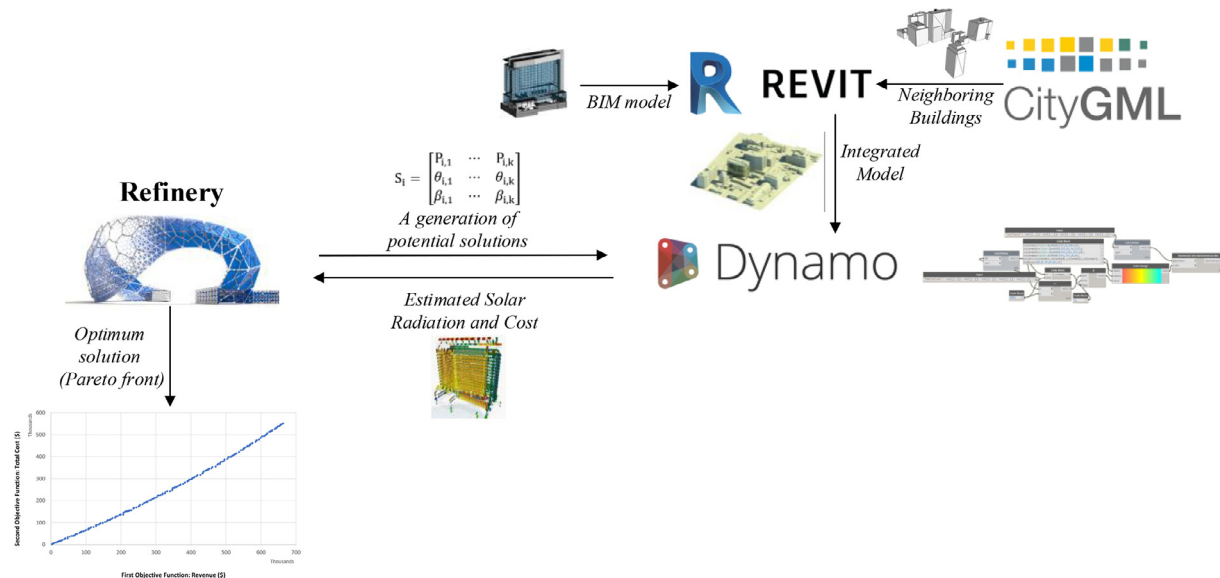
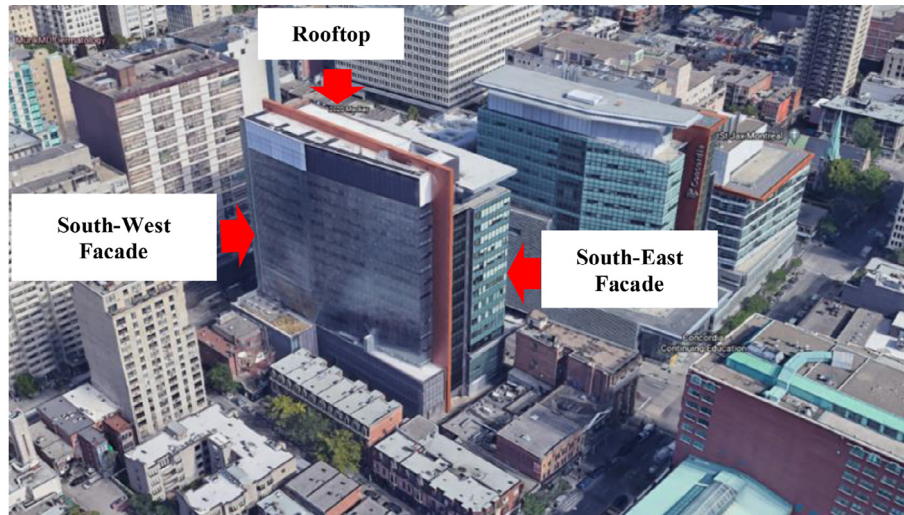
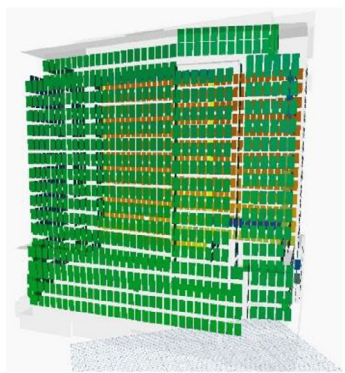


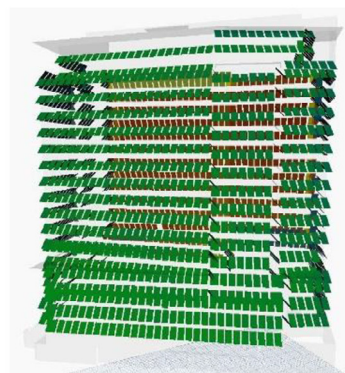
Fig. 6. Overview of the implementation.



(a)



(b)



(c)

Fig. 7. (a) John Molson School of Business, Concordia University [26], (b) and (c) radiation potential of north-east façade at 0° and 45° tilt angles, respectively (). Adapted from [47]

assumed as $r = 5\%$ and $g = 2.15\%$, respectively. To calculate the energy revenue, the average unit cost of electricity is considered $V = \$0.179$ per kWh (Electric [19]). The average cost of a PV module is assumed as $\$100/m^2$ [52]. The study period was considered 25 years (i.e. expected service life of the PV system). The maintenance cost is assumed as $\alpha = 0.5\%$ of the initial cost. It should be noted that for simplicity, it is assumed that the same type of PV module is used for all surfaces. Therefore, the same coefficients are applied to all cases. For more complex scenarios, this assumption can be easily adjusted in Dynamo.

4.2.1. Rooftop optimization scenarios

The grid size of the rooftop is generated for PV modules of $3\text{ m} \times 3\text{ m}$. This module size resulted in 120 potential points for the installation of panels. Three design scenarios are considered

for rooftop PV layout optimization, namely scenarios where PV modules have (1) Non-uniform orientation (i.e., each panel can have distinctive pan and tilt angles), (2) Uniform orientation (i.e., all panels have the same pan and tilt angles), and (3) Batched uniform orientation (i.e., a group of nearby panels all need to have same pan and tilt angles). In the batch uniform orientation scenario, all the panels with pair-wise Euclidean distances between their center points of less than a predefined threshold are bundled together as a batch. In this study, the threshold was set at 10 m, resulting in 7 distinctive groups of panels. The optimization configurations ($N = 60$ and $G = 60$) and the PV module size are fixed for all scenarios and are determined through several trials and errors. It was observed that the larger population size and number of generations would not result in significant improvement of the optimization performance. The optimization of the scenarios is done

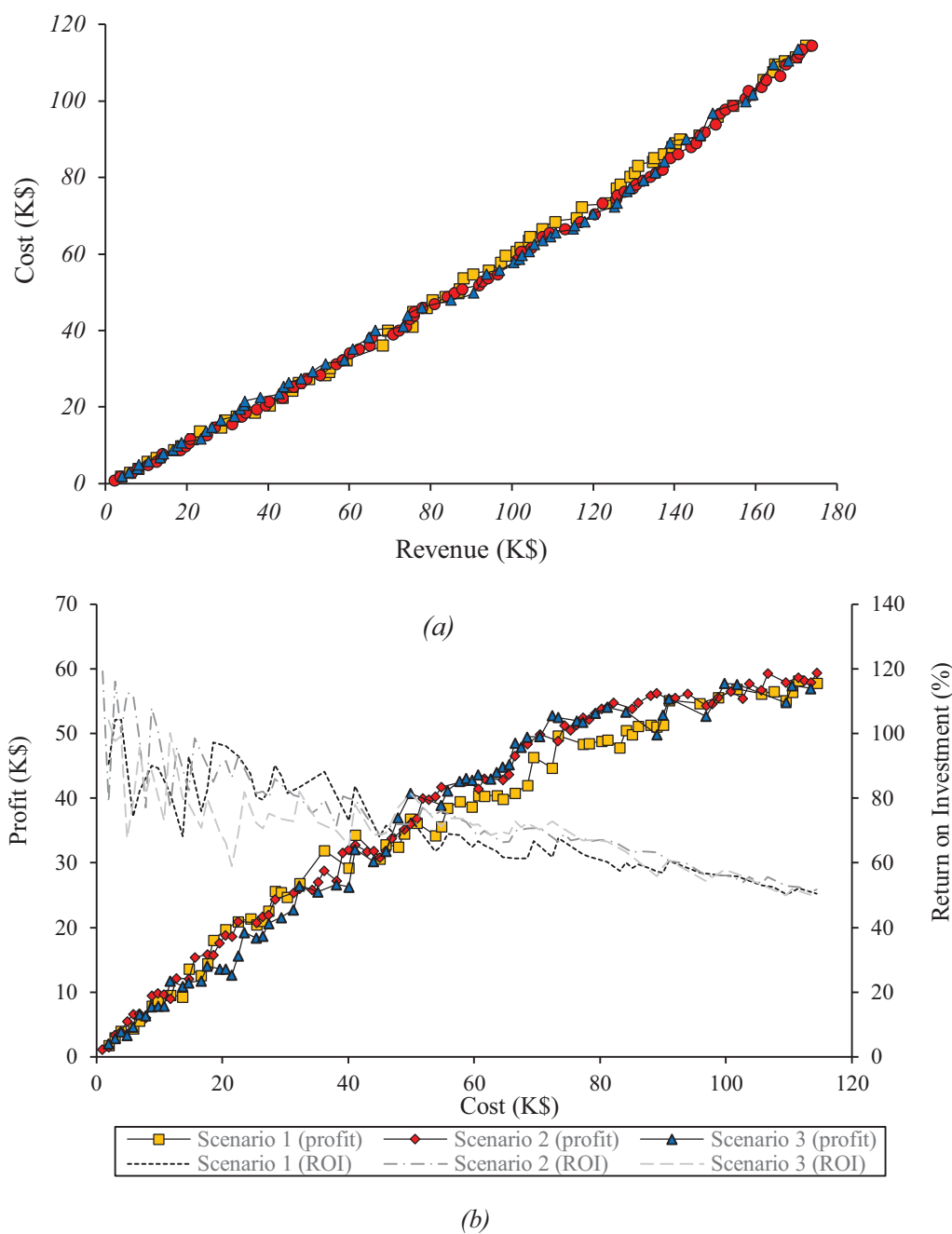


Fig. 8. (a) Pareto Fronts, (b) Cost vs. Profit and ROI of solutions of the three different scenarios.

considering all three input parameters as variables including $P_{i,k}$ (placement of PV modules), $\theta_{i,k}$ (tilt angle within the range of 0–90°), and $\beta_{i,k}$ (pan angle within the range of 0–360°).

Fig. 8(a) shows the Pareto fronts of near-optimum solutions for all three scenarios. As shown in this figure, the overlap between the Pareto fronts is significant. This suggests that all scenarios converged to rather similar solutions. There is a slight convex pattern between cost and revenue, suggesting that as the number of panels increases, the rate of revenue growth declines. This is logical because, at the lower number of panels, the panels are placed at locations where there is maximum radiation potential. By increasing the number of panels installed on the rooftop, panels have to be installed at the location with less radiation potential, resulting in the overall decline in revenue growth. To put this into perspective, **Fig. 8(b)** shows the overall cost vs profit of solutions of all three Pareto fronts. As shown in this figure, although the maximum profit is generated in cases where almost all panels are installed, Return on Investment (ROI) has a generally declining trend. **Table 2** provides a more detailed account of solutions with maximum profit in each of the scenarios and **Fig. 9** provides an overview of how these scenarios look like. These scenarios are compared to a

baseline scenario where all the panels are installed at the tilt and pan angles of 35° and 240°, respectively. The baseline case was derived from the sensitivity analysis performed in the previous work of the authors [47]. It is observed that all optimization scenarios offered better ROI than the baseline scenarios, with the minimum improvement being 8.5% for Scenario 2. While only two of the three scenarios generated higher revenue than the baseline scenarios, all three scenarios offered cost saving.

To investigate this further, the hypervolume values and indicators of the three Pareto fronts were calculated and compared using Eq. (5), as suggested by Salimi et al. [46]. Hypervolume indicator intends to compare several Pareto fronts coming from different scenarios and investigate which Pareto front is better in terms of finding more optimum solutions. In that sense, it is a metric used to evaluate the fitness of the optimization method across different scenarios (i.e., Pareto fronts). The hypervolume of each Pareto front is the area between a reference point (usually the maximum of the two objective functions in a minimization problem) and that Pareto front. The hypervolume indicator is then the ratio of the hypervolume of each Pareto front over the area between the reference point and the origin, as shown in Eq. (5).

Table 2
Maximum-profit solutions of the three scenarios for the rooftop design.

Rooftop PV design scenarios	Tilt [Mean, std] (Degree)	Pan [Mean, std] (Degree)	# of panels	Annual Cumulative Radiation (MWh)	Average Radiation (MWh/m ²)	Energy Revenue (KS)	Total Cost (KS)	Return on Investment (%)	Revenue improvement (compared to baseline) (%)	Cost improvement (compared to baseline) (%)
Baseline scenario	[35, 0]	[240, 0]	120	399	0.37	168.25	117.42	43.3	N/A	N/A
Non-uniform orientation	[45, 15]	[230, 18]	114	402.56	0.39	169.75	111.55	52.2	0.89	5
Uniform orientation	[45, 0]	[230, 0]	117	412.21	0.39	173.82	114.49	51.8	3.31	2.49
Batched uniform orientation	[50, 16]	[240, 35]	102	373.61	0.4	157.55	99.81	57.8	-6.36	15

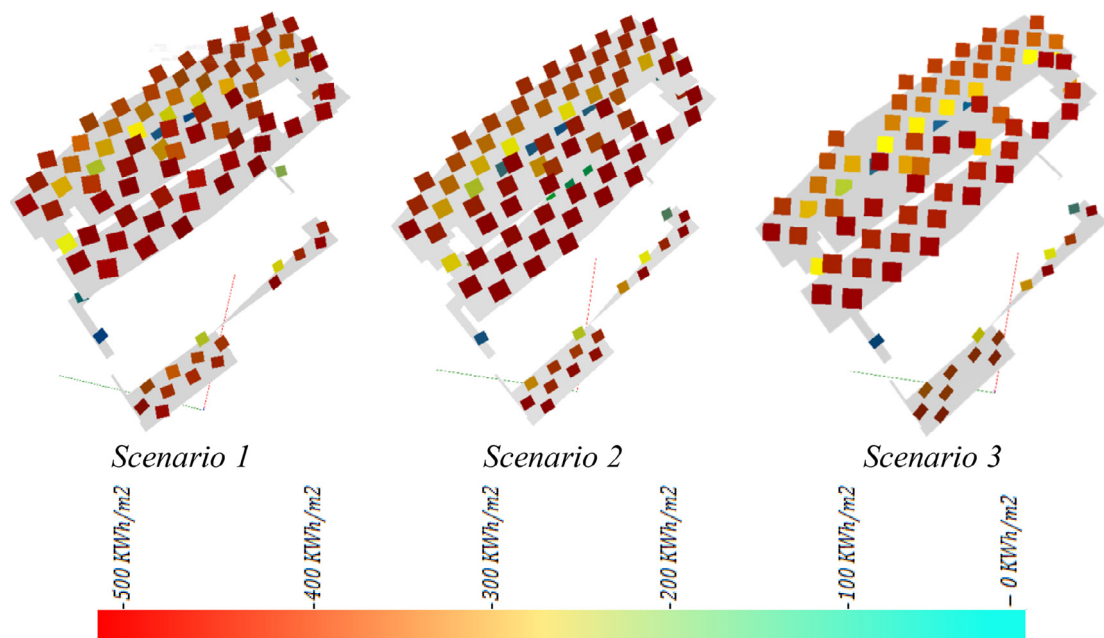


Fig. 9. Rooftop PV design scenario.

Table 3

Comparison of hypervolumes of the rooftop three Pareto fronts.

Scenario	Hypervolume Value (S^2)	Hypervolume indicator
Non-uniform orientation	1.029717×10^{10}	0.5377
Uniform orientation	1.048819×10^{10}	0.5476
Batched uniform orientation	1.034960×10^{10}	0.5404

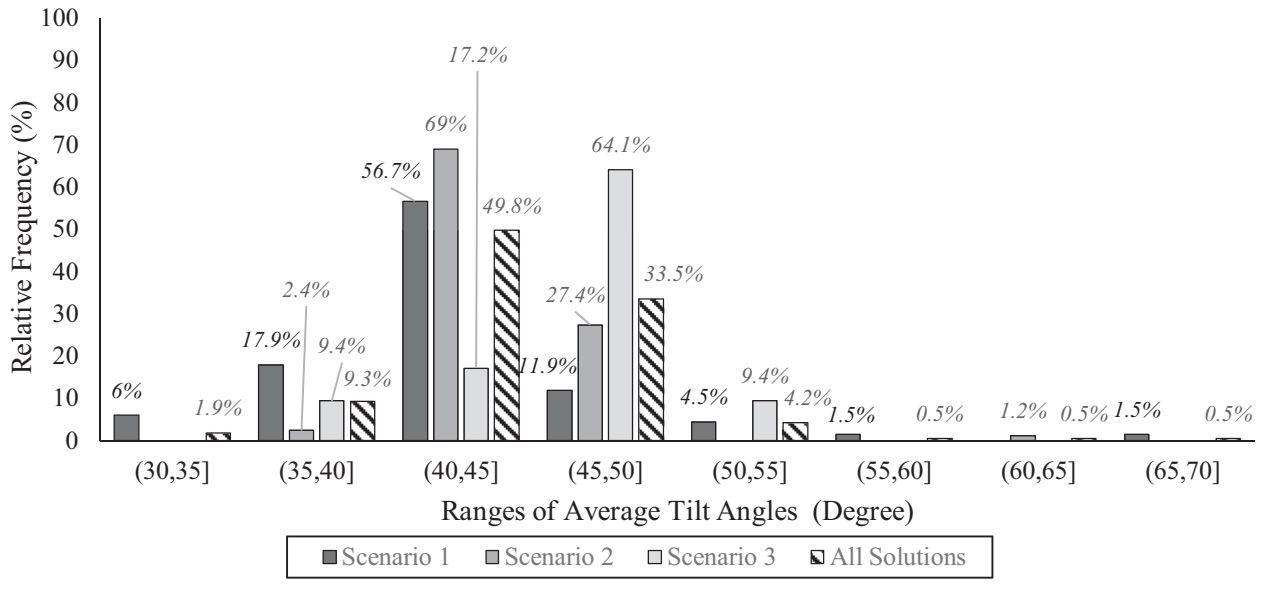
$$HI_{Par_1} = \frac{HV_{Par_1}}{(ObjectiveFunction1)_{Max} \times (ObjectiveFunction2)_{Max}} \times 100\% \quad (5)$$

Where: HV_{Par_1} : the hypervolume value of Pareto front I HI_{Par_1} : the hypervolume indicator of Pareto front I

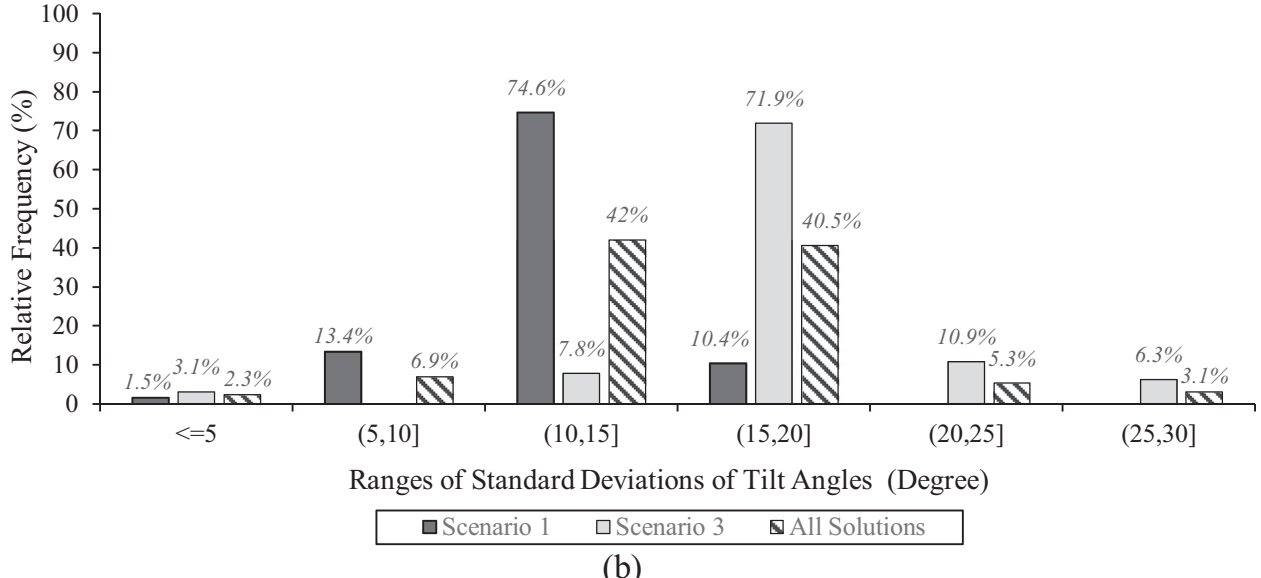
As shown in Table 3, the hypervolume indicators of all Pareto fronts are very close. This indicates that constraining the solutions

to uniformed angles and batching did not contribute to finding better solutions although the search spaces were reduced significantly. This can be an indication of the consistency and proper performance of the optimization module for even non-uniform orientation, where the search space is very large.

To further investigate the configuration of panels in all Pareto solutions of each scenario, the details of panel orientation were analyzed. Figs. 10 and 11 show the distributions of average tilt and pan angles in terms of the relative frequency of different angle ranges and their standard deviations. In addition to the distributions of the solutions of the three scenarios, the distributions of the pool of all solutions combined is also shown. As shown in Fig. 10(a), 92.6% of all the solutions (i.e., three Pareto fronts combined) have average tilt angles in the range of 35° to 50°. This is consistent with the theoretical optimum tilt angle for the Montreal region, which is 37° [31]. Fig. 10(b) suggests that in 89.4% of solutions the standard deviation of the tilt angle is between 5° to 20°. This represents a rather good uniformity of angles in scenarios where angle uniformity is not fully constrained. This can very well



(a)

**Fig. 10.** (a) The distribution of average tilt angles, (b) the standard deviation of angles (Rooftop).

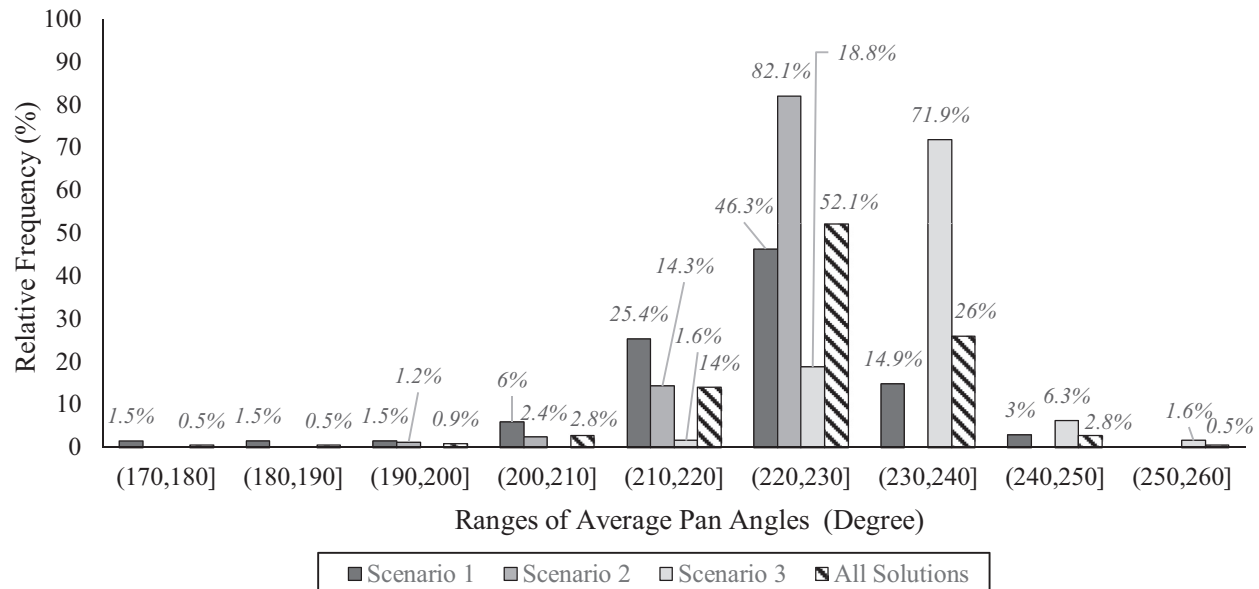
be construed as an indication that in general uniform patterns of tilt angles are preferred. This uniformity is more palpable in the first scenario, with 74.6% of solutions only having a standard deviation of 10° to 15°. This is mainly because in the third scenario, the batches are relatively further apart (compared to the first scenario) and this higher level of distinction results in higher variability in the tilt angle of panels. Another observation is that Scenario 2 has a considerably higher concentration of angles around 40° to 45°. This is because in this scenario all the panels have uniform angles and therefore the percentage of average angle becomes more concentrated. In all scenarios, the percentage of average angles of less than 35° and larger than 50° is very small.

Fig. 11 presents the analysis of the pan angles. As shown in this figure, again 92.1% of all the solutions have average pan angles of

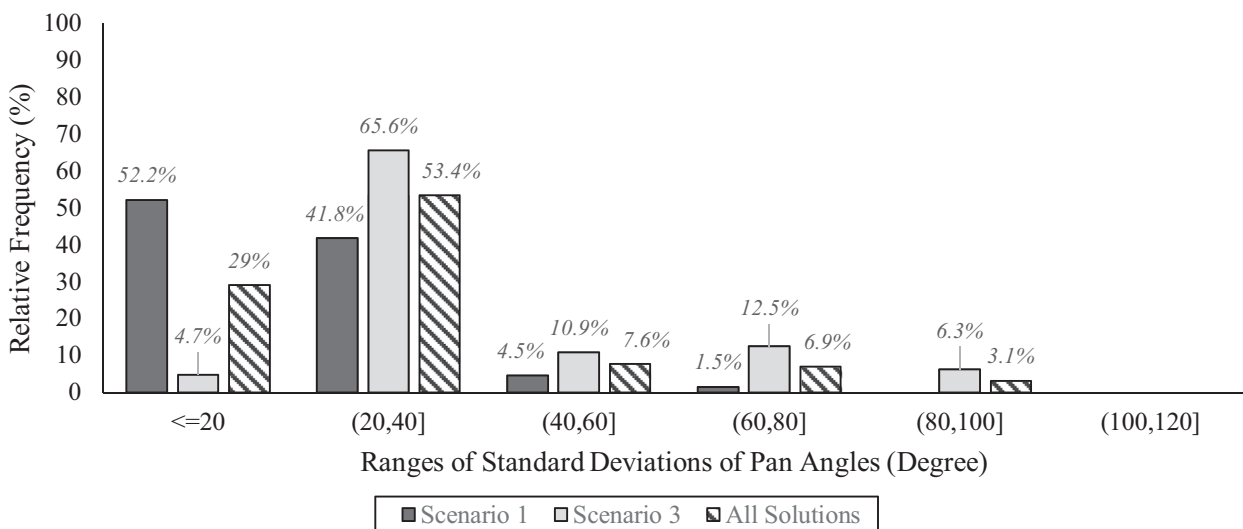
210° to 240°. Compared to tilt angles, pan angles demonstrate a higher degree of variability, with 82.4% of panels having a standard deviation of up to 40°. Again, consistent with the tilt angles, variability in the third scenario is higher than in the first scenario. Nevertheless, the results indicate that all panels are facing the same part of the sky (i.e., [180,270]).

4.2.2. Facade optimization scenarios

As explained in [Section 4.2](#), the South-West, North-West, and South-East of the facade surfaces were selected for the optimization process. To show the capability of the proposed BIM-based method to easily distinguish between various surfaces, only the installation of PV modules on the curtain walls was considered in this study. Based on the BIM model, the distance between two



(a)



(b)

Fig. 11. (a) The distribution of average pan angles, (b) the standard deviation of angles (Rooftop).

floors on the façade is covered by the curtain panels of 4 m high and 2 m wide. It is assumed that 25% of the floor height is occupied by windows and the remaining part is made of opaque panels. With this assumption, PV modules with the width of 1.5 m and height of 3 m were considered to be installed on the non-window part of each curtain wall, which resulted in a total of 1,137 locations for the installation of panels on the facade based on the generated grid. Four different scenarios were considered, i.e., (1) Non-uniform orientation, (2) Uniform orientation, (3) Batched uniform orientation, and (4) bounded tilt angles ($0 \sim 15^\circ$). In the case of batched uniform orientation, the batching of the panels was considered based on vertical clustering. In total, the entire height of the building was divided into 5 batches. Scenario 4 is considered because from the constructability perspective, it is preferred to install the PV modules as parallel to the vertical surface as possible. By limiting the amount of tilt angle

to the range of $0 \sim 15^\circ$, it is possible to analyze the extent to which the constructability concerns would compromise energy revenue.

The optimization configuration was set to ($N = 60$ and $G = 60$) and panel sizes were kept the same. As explained in Section 3.1, no pan angle was considered for the PV modules on the facade and therefore the optimization decision variables were only $P_{i,k}$ (placement of PV modules), $\theta_{i,k}$ (tilt angle within the range of $0 \sim 90^\circ$).

The Pareto front of the near-optimum solutions are shown in Fig. 12(a). Consistent with the observation of rooftop panels, there is a significant overlap between the solutions of the three scenarios. Again, the cost vs. revenue pattern is in a convex form. Fig. 12(b) shows the profit vs. cost relationship and ROI trend. Unlike the rooftop, the maximum profit for the facade did not happen at the maximum cost, suggesting that after a certain threshold, the cost of additional panels on the facade is not justified. This is

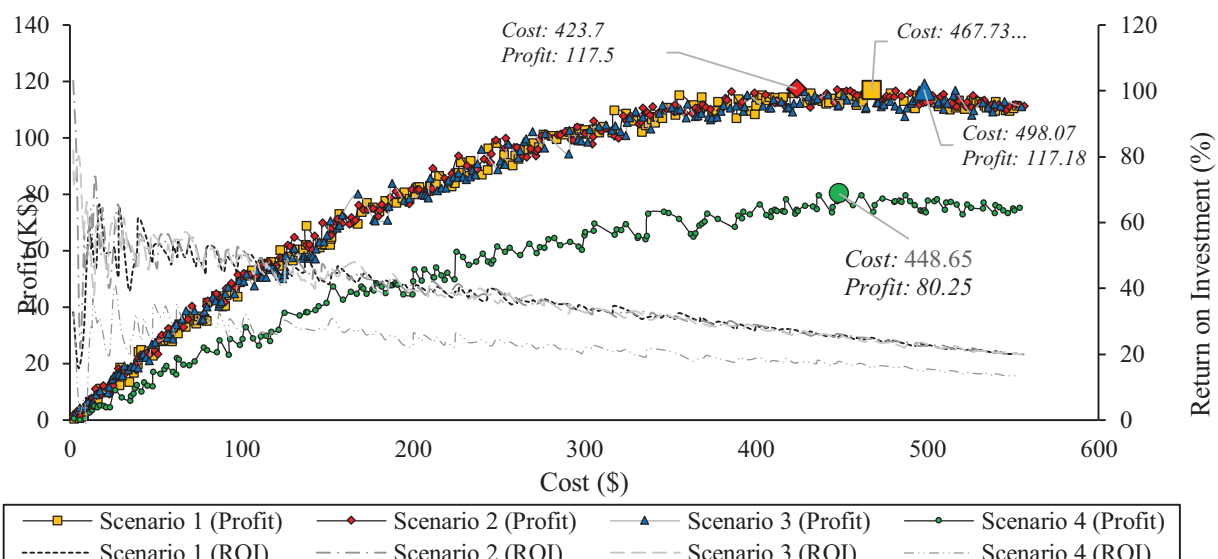
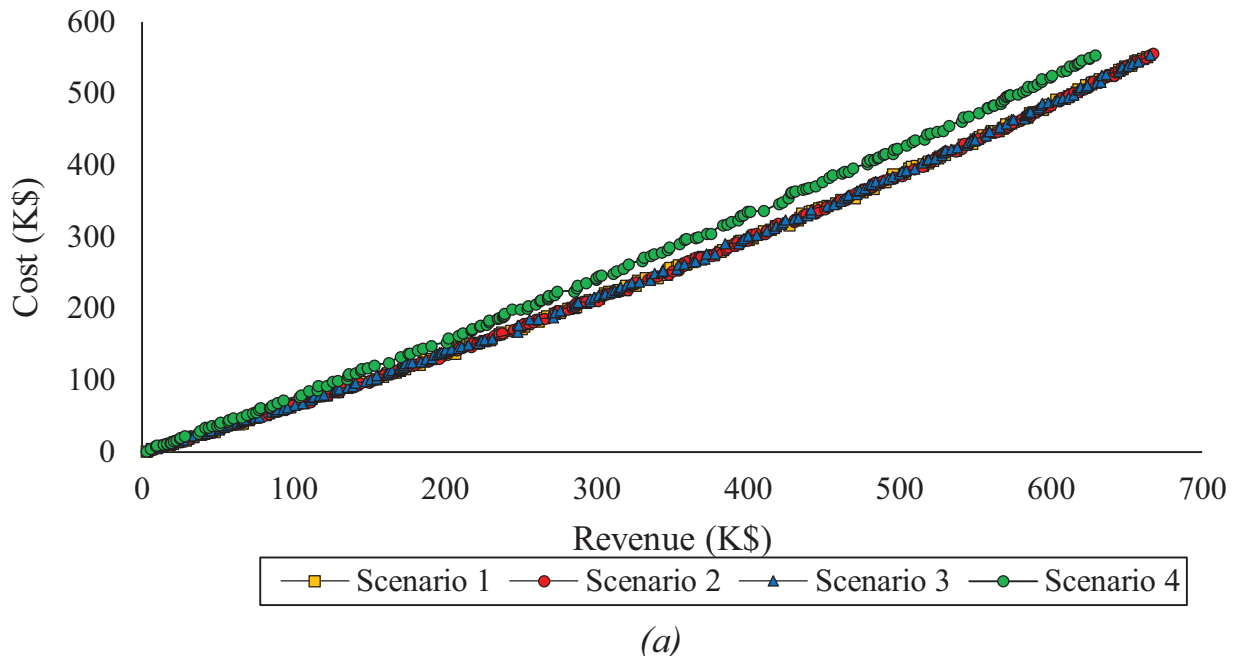


Fig. 12. (a) Pareto Fronts, (b) Profit vs. Cost and ROI of solutions of the three different scenarios (Facade).

because to achieve the full coverage of the curtain walls with PV modules, panels need to be installed at locations where there is not sufficient radiation potential. Therefore, compared to the rooftop, the facade tends to operate at a much lower ROI margin for the majority of solutions on the Pareto fronts. Again, this is a logical pattern because the radiation potential on the vertical surfaces is less than the horizontal surfaces, leading the solutions to yield less revenue for each panel installed. When the maximum-profit cases of the four scenarios are compared, it appears that Scenario 2 offers a slight advantage by offering a higher profit (\$117.5 K) for a lower cost (\$423.7 K) resulting in ROI of 27.7%. As demonstrated in Fig. 12, Scenario 4 generates palpably less revenue compared to other 3 scenarios. This is because unlike the other three scenarios where the panels could be at any tilt angle between $0 \sim 90^\circ$, in scenario 4 the panels are forced to remain within $0 \sim 15^\circ$ for improved constructability. Compared to the most profitable solution in Scenario 2, the best solution in Scenario 4 costs 6% more generates 32% less profit. This clearly suggests that limiting the tilt angles cause significant reduction in the profit.

Fig. 13 shows the layout of these four designs and Table 4 presents their details. When these scenarios are compared with the baseline case (i.e., PV panels are placed on all possible location without tilt angles), it is observed that all optimization scenarios offered solutions that are considerably cheaper for more or less similar energy revenue, as shown in Table 4. This highlights the significance and added value of the generative design approach towards PV installation.

Table 5 shows the hypervolume indicators of the Pareto fronts. As demonstrated, again there is no significant difference between the quality of the solutions offered by the first three scenarios. Again, scenario 4 is clearly worse than the other three scenarios. This suggests that constraining the problem had little contribution to improving the performance of the optimization module.

Similar to the case of rooftops, the configurations of PV modules on the Pareto fronts was analyzed and plotted in Fig. 14. Because Scenario 4 had a constraint on the tilt angle, it was excluded from this analysis. This figure represents the distribution of the averages of the tilt angles and the standard deviations of tilt angles of the solutions of all other three scenarios. As shown in Fig. 14(a), very similar to the case of the rooftop, the majority (i.e., 90.6%) of average tilt angles are between 35° to 50° . However, compared to the rooftop, the facade solutions tend to have lower tilt angles, with facade solutions having 31.7% of average tilt angles between 35° to 40° while this rate for the rooftop is only 9.3%. Again, the dominant tilt angles are consistent with the proposed theoretical values. The major difference between the facade and rooftop is the considerably lower variability of tilt angles in the case of the facade. As shown in Fig. 14(b), 86.1% of solutions have a standard deviation of less than 10° . In the case of the first scenario, 91% of solutions have a standard deviation of less than 5° . This suggests that Facade solutions are converging towards uniformity, far more than the rooftop.

4.2.3. Profit analysis for different study periods

In Sections 4.2.1 and 4.2.2, the optimization of the PV module layout was conducted for the fixed study period of 25 years. Also, the optimization was conducted as a multi-objective optimization that considered revenue and cost. However, different building owners may have different expectations in terms of when their investment needs to be paid back and, in many cases, their final decision is motivated by the generated profit. Essentially, the shorter the expected payback period, the smaller the number of PV modules that need to be considered in order to maximize the profit. To test this hypothesis, the first scenario of non-uniform orientation of panels on the facade was taken to investigate the impact of changing the study period on the optimum solution from

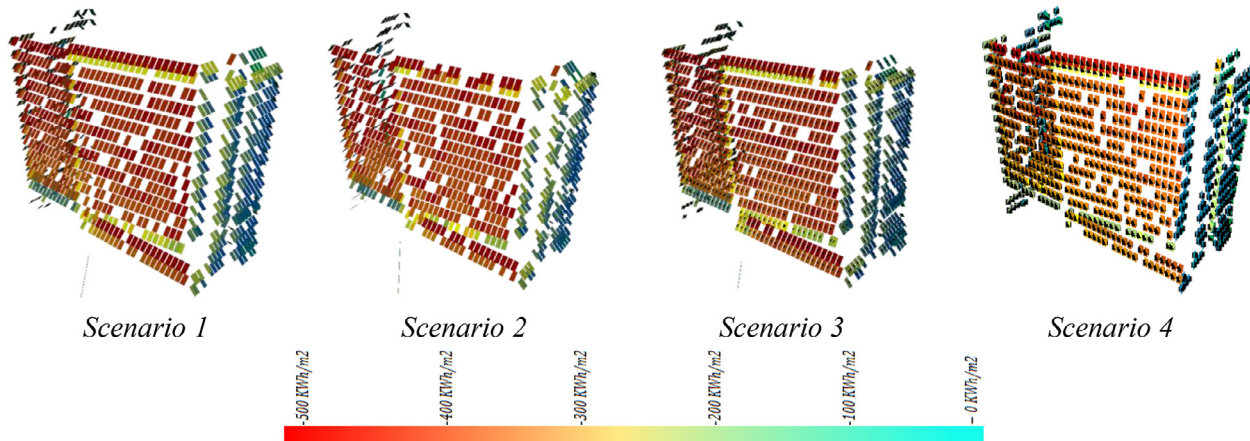


Fig. 13. Facade PV design scenarios.

Table 4

Maximum-profit solutions of the three scenarios for the facade design.

Rooftop PV design scenarios	Tilt [Mean, std] (Degree)	# of panels	Annual Cumulative Radiation (MWh)	Average Radiation (MWh/m ²)	Energy Revenue (KS)	Total Cost (KS)	Return on Investment (%)	Revenue improvement (compared to baseline) (%)	Cost improvement (compared to baseline) (%)
Baseline Scenario	[0, 0]	1137	1360.44	0.26	573.67	556.29	3.12	N/A	N/A
Non-uniform orientation	[45, 2]	956	1386.12	0.32	584.50	467.73	25	1.89	15.92
Uniform orientation	[45, 0]	866	1283.43	0.33	541.20	423.70	27.7	-5.66	23.83
Batched uniform orientation	[40, 4]	1018	1459.06	0.32	615.25	498.07	23.5	7.25	10.47
Bounded tilt angles ($0 \sim 15^\circ$)	[15, 2]	917	1254.28	0.30	528.90	448.65	17.9	-7.80	19.34

Table 5

Comparison of hypervolumes of the facade three Pareto fronts.

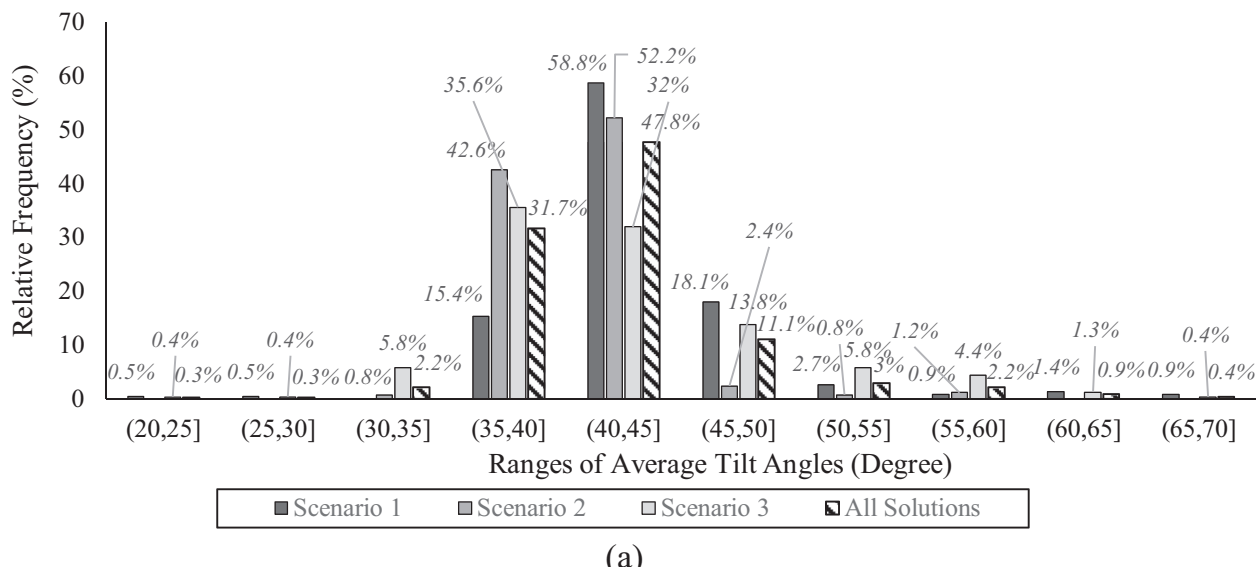
Scenario	Hypervolume Value (\$^2)	Hypervolume indicator
Non-uniform orientation	1.99306×10^{11}	0.5406
Uniform orientation	1.99744×10^{11}	0.5418
Batched uniform orientation	1.98959×10^{11}	0.5397
Bounded tilt angles (0 ~ 15°)	1.82400×10^{11}	0.4948

the profit perspective. To do so, the multi-objective problem of the previous sections was replaced with a single-objective problem that aims to only maximize profit. Therefore, each optimization run yields a single near-optimum design that maximizes the profit of the building owner. Five different study periods were considered, namely 5, 10, 15, 20, and 25 years. The results are presented in Table 6 and Fig. 15. It should be highlighted that, as can be seen in Table 6, the solution with the maximum profit for the study period of 25 years is different from the results shown in Table 4. This is because the previous optimization was not searching for the maximum-profit solutions, but rather for maximum revenue and

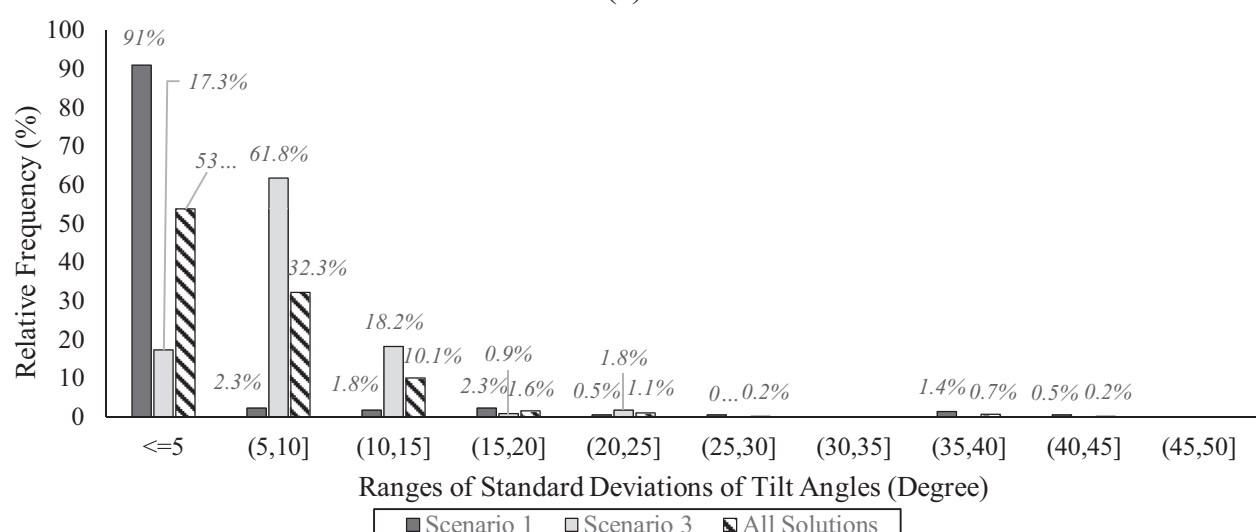
minimum cost. As can be discerned from the comparison of Tables 4 and 6, when the optimization is changed to a single-objective problem focusing on maximizing profit, the identified solution performs better, albeit marginally. As shown in Table 6, there is no profit for the first five years of the project even with a minimum number of PV modules. By considering the longer study period, the number of applied PV modules can increase and the project starts to make a profit. As shown in this table, the longer the study period, the higher the ROI and the more profitable the project becomes.

4.2.4. Analysis of the impact of PV module size on self-shadowing

As discussed in Section 3, the self-shadowing effect of PV modules needs to be taken into account when considering their use on the buildings' facade. To test this hypothesis, the optimization of facade PV layout was done for three different heights of PV panels, namely, panels with the size of $1.5 \text{ m} \times 2 \text{ m}$, $1.5 \text{ m} \times 3 \text{ m}$, and $1.5 \text{ m} \times 4 \text{ m}$ with the same grid spacing. In this case, the problem was defined as a multi-objective optimization problem with the objectives to maximize the revenue and minimize the cost.



(a)



(b)

Fig. 14. (a) The distribution of average tilt angles, (b) the standard deviation of angles (Facade).

Table 6

Profit for different study periods.

Study Period (Years)	Average Tilt angle (Degree)	# of panels	Revenue (KS)	Total Cost (KS)	Return on Investment (%)
25	40	856	537.96	418.81	28.4
20	40	667	374.62	322.44	16.2
15	50	115	63.26	54.82	15.4
10	45	4	2.03	1.88	8.5
5	50	4	1.08	1.84	-41.3

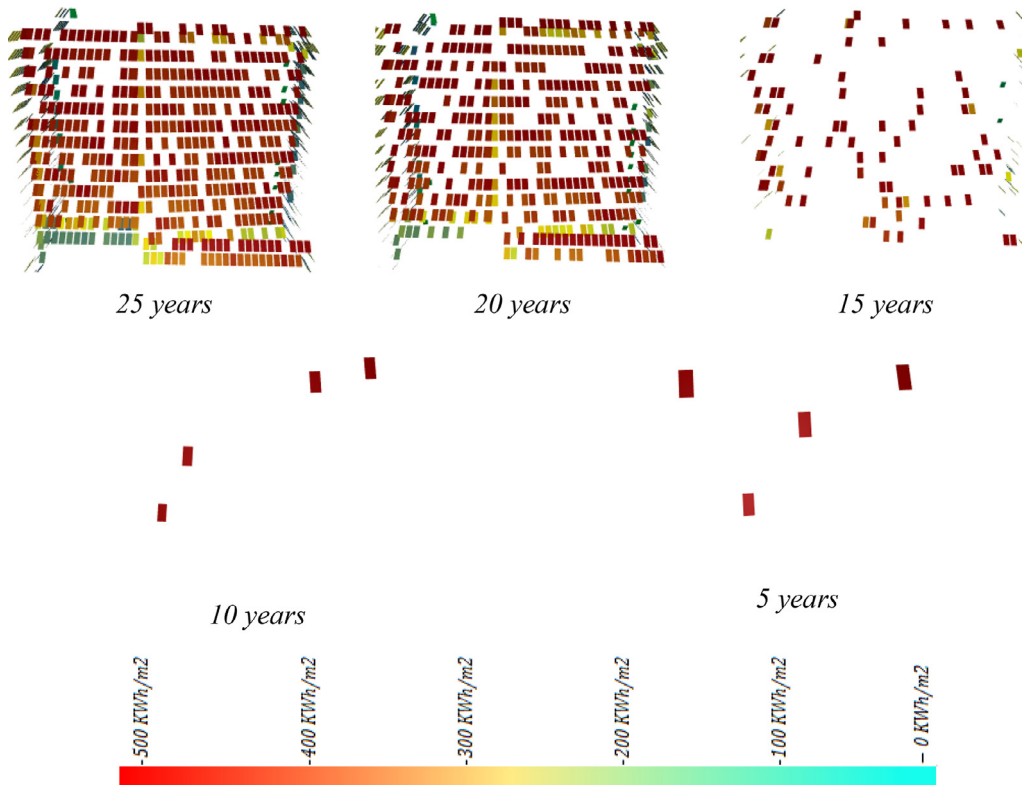
**Fig. 15.** Facade PV modules for different study periods.

Fig. 16 presents the results of this optimization. The details of the most profitable solutions of each scenario are presented in **Table 7** and **Fig. 17**.

The main observation in this analysis is that the maximum profit is achieved when $1.5 \text{ m} \times 3 \text{ m}$ panels are used. This is because while smaller panels do not exploit the full potentials of the vertical surfaces, i.e., by covering less area, the performance of PV systems with larger panels is compromised by the increased chance of self-shadowing.

Also, as shown in **Fig. 16(a)**, as the size of panels increases, the cost of the overall solution also increases. However, the profit does not continuously increase along with the increasing panel sizes. As shown in this figure, the ROIs of different solutions remain almost the same with respect to changes to the panel size. This means that by increasing the panel size, the cost and revenue increase almost at the same rate. The main difference between panel sizes is that although the ROI remains almost intact when the panel sizes are increased, the same profit can be generated by using a smaller number of panels, as shown in **Fig. 16(b)**.

When analyzing the optimum tilt angles of these scenarios, it appears that the panel size does not have a significant impact on the optimal orientation of panels. The average tilt angles and their standard deviation are [46.6, 4.3], [46.2, 3.3], and [47.7, 3.6] for 1.

$5 \text{ m} \times 2 \text{ m}$, $1.5 \text{ m} \times 3 \text{ m}$, $1.5 \text{ m} \times 4 \text{ m}$ sizes, respectively. Again, the optimum tilt angle is consistent with the theoretical recommendations.

5. Discussions

The present paper made a novel contribution to the body of knowledge by presenting a BIM-based generative design framework for PV module layout design on the whole exterior of high-rise buildings. The main novelty of this framework is that by deploying the semantics of the BIM model, PV layout optimization can be done at a surface-specific level, allowing designers to consider the complex interaction between building surface types (e.g., windows, walls, etc.), type of PV module (e.g., opaque, semi-transparent, etc.), their tilt and pan angles, and the financial aspect of the PV system (i.e., revenue vs. cost at different study periods). The parametric model developed in the previous work of the authors was seamlessly integrated with an optimization platform to enable a streamlined generative design of the PV module layout.

The proposed generative design optimization method can be used to analyze the feasibility of installing BIPV on the façade of

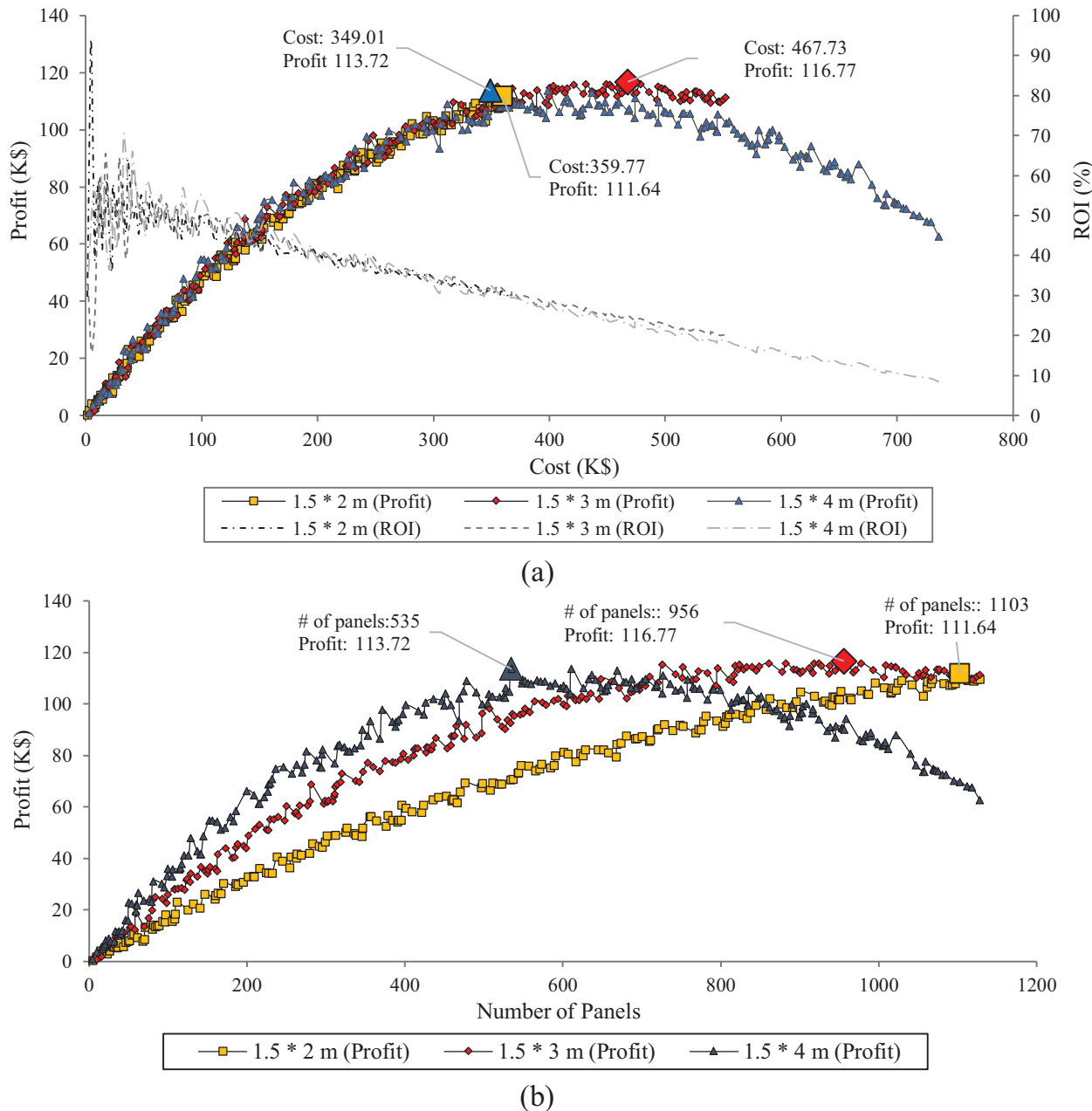


Fig. 16. (a) Cost vs. Profit and ROI, (b) number of panels vs. profit of solutions of the three different scenarios with different sizes of panels.

Table 7

Comparing three different sizes of PV modules to show the self-shadow effect.

PV module size (m^2)	Tilt [Mean, std] (Degree)	# of panels	Annual Cumulative Radiation (MWh)	Average Radiation (MWh/m^2)	Revenue (K\$)	Total Cost (K\$)	Return on Investment (%)
1.5 * 2	[40,1]	1103	1117.93	0.33	471.41	359.77	31
1.5 * 3	[45,2]	956	1386.12	0.32	584.50	467.73	25
1.5 * 4	[40,2]	535	1097.35	0.34	462.73	349.01	33

newly designed buildings as well as retrofitting the facades of existing buildings. In both cases, the detailed BIM model of the building envelope is required. For this purpose, the following levels of detail (LOD) can be considered: (a) LOD 350 (Construction Documentation), which represents how building elements (e.g. curtain walls) interface with each other, (b) LOD 400 (Fabrication and Assembly), which has the precise dimensions and location of building envelope, and (c) LOD 500 (As-Built), in which the elements are

modeled as constructed for maintenance and operations. The LOD 350 is more suitable in the case of new newly designed building while the LOD 400 and 500 can be available only in the case of existing buildings. In the case that the BIM model of an existing building is not available, the model can be created using LiDAR scan-to-BIM methods (e.g. [62]).

As explained in the previous work of the authors [47], the proposed method can be integrated with the Architecture, Engineering

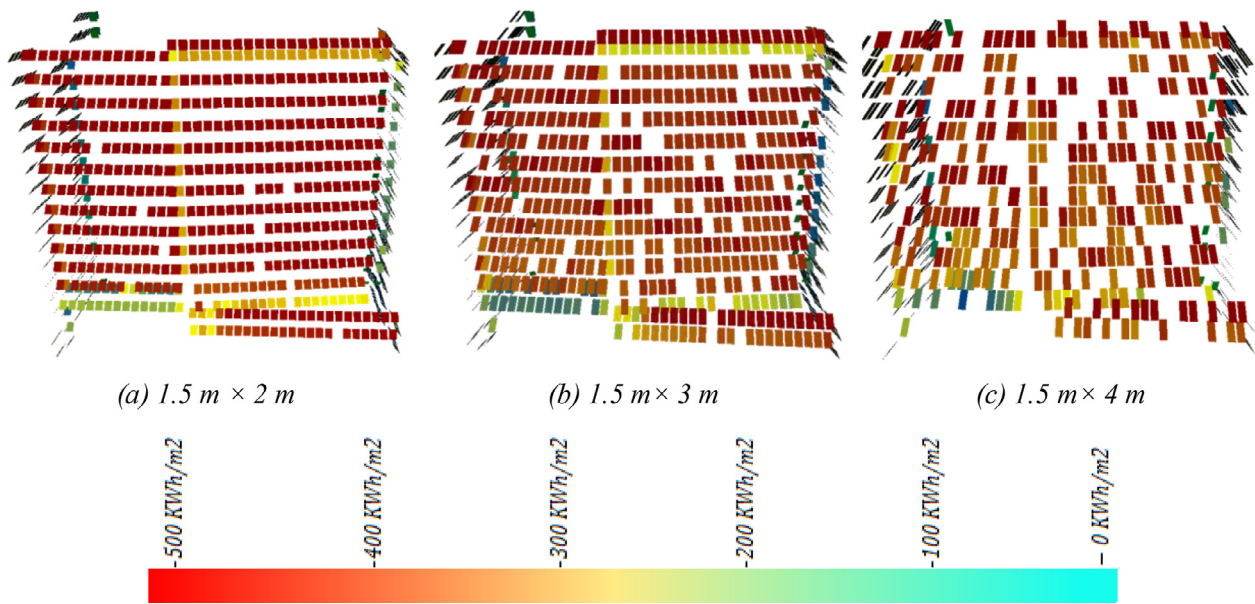


Fig. 17. Optimum PV layouts with three different module sizes.

and Construction (AEC) processes at different phases. In the case of a newly designed building, the designers can use the results of the optimization PV module layout (Pareto front solutions) to compare different alternatives and to discuss with the decision makers (e.g. developer, owner) about the best configuration based on the design requirements and constraints (i.e. energy efficiency, esthetic, budget, expected payback period). In the case of retrofitting an existing building, a similar approach can be used taking into consideration the additional constraints of the current structure. The most important insight generated by the elaborate case study presented in Section 4 is that while the authors have hypothesized that to gain an optimum yield of the PV system on the facade of buildings, the tilt angles of different arrays of panels need to vary, it was demonstrated that in the majority of the studied scenarios, the optimum solutions favored a more consistent orientation of the panels. The optimum average tilt angles of panels are very much consistent with the theoretical and heuristic recommendations. Nevertheless, it is shown that the high variation of pan angles of PV modules on the horizontal surfaces improves the performance of the PV system. From the aesthetic and installation standpoint, this is more acceptable than the variability in the vertical PV modules because PV modules on horizontal surfaces are less visible and more accessible.

It is also shown that the maximum profit does not always occur when there is a maximum revenue. The installation of panels on any possible location will generate revenue over time; however, if the radiation potential is low, the cost could exceed the revenue and thus push the entire design away from financial optimality. However, it is shown that the expected time horizon for ROI has a major impact on how the optimum PV layout looks and which potential installation locations need to be leveraged. The longer the ROI horizon, the more PV modules can be considered for the installation because even locations with lower radiation potential can become profitable after a certain period of time. This was clearly demonstrated in Section 4.2.3.

Finally, it was demonstrated that the size of the PV modules has some impact on the optimum layout. The larger the panel sizes, the greater the chance of reduced yield because of the self-shadowing effect but also the higher the amount of energy generated by the panel. Overall, the rate of energy harvested per m^2 of panels

changes marginally with the increased size of panels. Nevertheless, given that smaller panels cannot exploit the full potentials of the vertical surfaces and the larger panels have a self-shadow effect, there seems to be a sweet spot in terms of the panel sizes, where the maximum profit can be generated. The proposed framework can help find the optimum size for each building.

6. Summary, conclusions and future works

This paper proposed a BIM-based generative design approach to optimize the PV modules layout on the building skin. After developing a surface-specific solar radiation simulation model for the building surfaces, an optimization module is integrated with the simulation platform to satisfy two objective functions in the design scenarios. Ultimately, the optimal layout of the PV modules aims to maximize the energy revenue and minimize the life cycle cost. A case study is presented for a high-rise building in Montreal, Canada. Various optimization design scenarios are generated for the rooftop and facade surfaces. Comparing the optimization results for different design scenarios for the rooftops and facades reveals that having a more uniform arrangement in PV layout design increases the chance of using the full capacity of the surface for the installation, because of increasing the generated energy due to less self-shadow effect. In addition to increasing energy revenue, the unified arrangement of the PV modules on the target faced surfaces (i.e. Scenario 2) improves the aesthetic value of the PV layout design and reduces the installation and technical complications.

Since measuring the economic benefit is usually a key step for the building owners and the investors, to investigate the project profit for different study periods, a single objective optimization is conducted to maximize the profit. The results show that the number of the PV modules and the project profit are increased by considering a longer study period.

Based on the above results, it can be concluded that the integration of the surface-specific simulation with the optimization using the generative design approach enables the decision-makers and the investors to consider multiple variables in the design process and find out the optimum solutions based on their needs. The comparison of the results of optimization with the baseline cases

indicates the added value of performing optimization for the PV layout design. Overall, a more consistent configuration of PV module is more optimal especially on the façade. It is also discerned that the longer the study period, the more solar panels can be considered for the installation and the higher the return on investment. Also, it appears that constraining the optimization problem, by introducing restrictions on the decision variables, has little impact on the optimality of the solutions identified by the generative design.

However, there are still some limitations in the research that can be addressed in the future. First, due to the lack of control on the hyperparameters of the optimization engine (i.e., Refinery platform) the current optimization process is slow. It can be envisioned that by further improvement of this platform or by replacing it with a more open-source alternative, the optimization process can be further enhanced. Second, although the panel size was considered, it was not incorporated as a decision variable. Considering varying panel sizes in a single solution can potentially generate more favorable solutions. Third, although the BIM-based nature of the proposed method offers the apparatus for multi-PV-modules solutions, this research only considered one type of PV module at a time. This can be changed in the future to better consider the practicality and aesthetic aspects of PV layout design. Fourth, in the case study, the same costing model is used for all the PV modules because the PV modules are installed on the vertical curtain walls. However, because the developed framework is surface-specific, it is very easy to customize the cost model to consider the variations of the costs of PV modules installed on different surfaces and with different configurations. Future studies should consider different cost models depending on the type of panels, configuration (e.g. a ventilated façade, curtain wall, window, etc.), and accessibility of the panel for maintenance. In addition, the cost variations of installing the PV modules on the facades with different tilt angles should be considered in future work. The cost model can be improved by introducing a coefficient for the difficulty of construction based on the standard deviation of all panels (i.e., the higher the standard deviation, the higher the cost of installation). This would require detailed field study on the actual construction cost of various PV configurations. Fifth, the current case study considered the installation of PV modules as a design step subsequent to the design of the facade. It can be argued that the design of the facade itself can also be optimized considering the solar radiation potentials. This can be considered in the future research.

Declaration of Competing Interest

The authors declare that they have no known competing financial interests or personal relationships that could have appeared to influence the work reported in this paper.

References

- [1] S.A. Al-Janahi, O. Ellabban, S.G. Al-Ghamdi, A Novel BIPV reconfiguration algorithm for maximum power generation under partial shading, *Energies* 13 (17) (2020) 44–70.
- [2] ArcGIS, 2021. Esri. Retrieved from <http://www.esri.com/software/arcgis/arcgis-for-desktop>
- [3] D. Attoye, K. Tabet Aoul, A. Hassan, A review on building integrated photovoltaic façade customization potentials, *Sustainability* 9 (12) (2017) 1–24.
- [4] Autodesk, Introduction to Generative Design Retrieved from Refinery Primer: <https://refineryprimer.dynamobim.org/01-introduction>, 2021.
- [5] Autodesk, Project Refinery Retrieved from <https://dynamobim.org/project-refinery-0-62-2-now-available/>, 2021.
- [6] Autodesk, Revit Retrieved from <http://www.autodesk.com/education/free-software/revit>, 2021.
- [7] M.C. Brito, N. Gomes, T. Santos, J.A. Tenedório, Photovoltaic potential in a Lisbon suburb using LiDAR data, *Sol. Energy* 86 (1) (2012) 283–288.
- [8] L. Brown, The Great Transition: Shifting from Fossil Fuels to Solar and Wind Energy. Washington, D.C: W. W. Norton Company, 2015. doi:0393351149, 9780393351149
- [9] L. Bueno, M. Ibliba, B. Vizcarra, G.M. Chaudhry, M.K. Siddiki, in: Feasibility analysis of a solar photovoltaic array integrated on façades of a commercial building, IEEE, 2015, pp. 1–4.
- [10] I. Caetano, L. Santos, A. Leitão, Computational design in architecture: Defining parametric, generative, and algorithmic design, *Front. Architect. Res.* 9 (2) (2020) 287–300.
- [11] B. Celik, E. Karatepe, S. Silvestre, N. Gokmen, A. Chouder, Analysis of spatial fixed PV arrays configurations to maximize energy harvesting in BIPV applications, *Renew. Energy* 75 (2015) 534–540.
- [12] C.L. Cheng, C.S. Sanchez Jimenez, M.-C. Lee, Research of BIPV optimal tilted angle, use of latitude concept for south orientated plans, *Renew. Energy* 34 (6) (2009) 1644–1650.
- [13] City of Montreal, Maquette numérique (Bâtiments CityGML LOD2 avec textures) Retrieved from Portail des données ouvertes: <http://donnees.ville.montreal.qc.ca/>, 2021.
- [14] P. Corti, L. Capannolo, P. Bonomo, p. De Berardinis, F. Frontini, Comparative Analysis of BIPV Solutions to Define Energy and Cost-Effectiveness in a Case Study, *Energies* 13 (15) (2020) 3827, <https://doi.org/10.3390/en13153827>.
- [15] J.d.S. Freitas, J. Cronemberger, R.M. Soares, C.N.D. Amorim, Modeling and assessing BIPV envelopes using parametric Rhinoceros plugins Grasshopper and Ladybug, *Renewable Energy* 160 (2020) 1468–1479.
- [16] V. Delisle, M. Kummert, Cost-benefit analysis of integrating BIPV-T air systems into energy-efficient homes, *Sol. Energy* 136 (2016) 385–400, <https://doi.org/10.1016/j.solener.2016.07.005>.
- [17] Dynamo, Open source graphical programming for design Retrieved from <http://dynamobim.org/>, 2021.
- [18] R. Eke, C. Demircan, Shading effect on the energy rating of two identical PV systems on a building façade, *Sol. Energy* 122 (2015) 48–57.
- [19] Electric Choice, 2021. Retrieved from <https://www.electricchoice.com/electricity-prices-by-state/>
- [20] R. Erdélyi, Y. Wang, W. Guo, E. Hanna, G. Colantuono, Three-dimensional SOLAR RADiation Model (SORAM) and its application to 3-D urban planning, *Sol. Energy* 101 (2014) 63–73.
- [21] F. Formulas, Present Value of a Growing Annuity Retrieved from http://financeformulas.net/Present_Value_of_Growing_Annuity.html, 2021.
- [22] S. Freitas, M.C. Brito, Maximizing the solar photovoltaic yield in different building facade layouts. (pp. 14–18). Hamburg, Germany: In Proceedings of the European Photovoltaic Solar Energy Conference and Exhibition, 2015.
- [23] S. Freitas, F. Serra, M.C. Brito, PV layout optimization: String tiling using a multi-objective genetic algorithm, *Sol. Energy* 118 (2015) 562–574.
- [24] Fu, R., Feldman, D., Margolis, R., woodhouse, M., & Ardani, K. (2017). U.S. Solar Photovoltaic System Cost Benchmark: Q1 2017. National Renewable Energy Laboratory.
- [25] H. Gholami, H. Røstvik, Economic analysis of BIPV systems as a building envelope material for building skins in Europe, ISSN 0360-5442 *Energy* 204 (2020) 117931, <https://doi.org/10.1016/j.energy.2020.117931>.
- [26] Google Earth, (2021). Retrieved from <https://earth.google.com>
- [27] Hagerty, K., & Cormican, J. (2019). Components for solar panel (PV) system. Retrieved from altestore.com: <https://www.altestore.com/howto/components-for-your-solar-panel-photovoltaic-system-a82/>
- [28] T. Hong, C. Koo, J. Park, H.S. Park, A GIS (geographic information system)-based optimization model for estimating the electricity generation of the rooftop PV (photovoltaic) system, *Energy* 65 (2014) 190–199.
- [29] T. Hwang, S. Kang, J.T. Kim, Optimization of the building integrated photovoltaic system in office buildings—Focus on the orientation, inclined angle and installed area, *Energy Build.* 46 (2012) 92–104.
- [30] Irena, Clean Energy Corridors Retrieved from International Renewable Energy Agency: <https://www.irena.org/cleanenergycorridors>, 2021.
- [31] M.Z. Jacobson, V. Jadhav, World estimates of PV optimal tilt angles and ratios of sunlight incident upon tilted and tracked PV panels relative to horizontal panels, *Sol. Energy* 169 (2018) 55–66.
- [32] T. James, A. Goodrich, M. Woodhouse, R. Margolis, S. Ong, Building-Integrated Photovoltaics (BIPV) in the Residential Sector: An Analysis of Installed Rooftop System Prices, Technical Report NREL/ TP-6A20-53103, Golden, Colorado. (2011), <https://doi.org/10.2172/1029857>.
- [33] M. Karteris, T.h. Slini, A.M. Papadopoulos, Urban solar energy potential in Greece: A statistical calculation model of suitable built roof areas for photovoltaics, *Energy Build.* 62 (2013) 459–468.
- [34] C. Koo, T. Hong, M. Lee, J. Kim, An integrated multi-objective optimization model for determining the optimal solution in implementing the rooftop photovoltaic system, *Renew. Sustain. Energy Rev.* 57 (2016) 822–837.
- [35] S. Kucuksari, A.M. Khaleghi, M. Hamidi, Y.e. Zhang, F. Szidarovszky, G. Bayraksan, Y.-J. Son, An Integrated GIS, optimization and simulation framework for optimal PV size and location in campus area environments, *Appl. Energy* 113 (2014) 1601–1613.
- [36] Ladybug Tools. (2021). Retrieved from <https://www.ladybug.tools/ladybug.html>
- [37] Y. Li, C. Liu, Techno-economic analysis for constructing solar photovoltaic projects on building envelopes, *Build. Environ.* 127 (2018) 37–46.
- [38] Q. Lin, K. Kensek, M. Schiler, J. Choi, Streamlining sustainable design in building information modeling BIM-based PV design and analysis tools, *Architect. Sci. Rev.* 64 (6) (2021) 467–477.

- [39] S. Liu, X. Meng, C. Tam, Building information modeling based building design optimization for sustainability, *Energy Build.* 105 (2015) 139–153.
- [40] LunchBox. (2021). Retrieved from proving ground: <https://provingground.io/tools/lunchbox/>
- [41] V. Mallawaarachchi, Towards Data Science Retrieved 2018, from <https://towardsdatascience.com/>, 2021.
- [42] E.G. Melo, M.P. Almeida, R. Zilles, J.A.B. Grimon, Using a shading matrix to estimate the shading factor and the irradiation in a three-dimensional model of a receiving surface in an urban environment, *Sol. Energy* 92 (2013) 15–25.
- [43] G. Ning, L.i. Junnan, D. Yansong, Q. Zhifeng, J. Qingshan, G. Weihua, D. Geert, BIM-based PV system optimization and deployment, *Energy Build.* 150 (2017) 13–22.
- [44] G. Ning, H.e. Kan, Q. Zhifeng, G. Weihua, D. Geert, e-BIM: a BIM-centric design and analysis software for Building Integrated Photovoltaics, *Autom. Constr.* 87 (2018) 127–137.
- [45] Rhinoceros. (2021). Retrieved from <https://www.rhino3d.com/6/new/grasshopper/>
- [46] S. Salimi, M. Mawlana, A. Hammad, Performance analysis of simulation-based optimization of construction projects using high performance computing, *Autom. Constr.* 87 (2018) 158–172.
- [47] N. Salimzadeh, F. Vahdatikhaki, A. Hammad, Parametric Modelling and Surface-specific Sensitivity Analysis of PV Module Layout on Building Skin Using BIM, *Energy Build.* 216 (2020) 109953.
- [48] SEIA. (2019). Solar Means Business.
- [49] Simulation and design of solar systems. (2021). Retrieved from photovoltaic-software.com: <https://photovoltaic-software.com/principle-ressources/how-calculate-solar-energy-power-pv-systems>
- [50] V. Singh, N. Gu, Towards an integrated generative design framework, *Des. Stud.* 33 (2) (2012) 185–207.
- [51] Solar Analysis. (2021). Retrieved from Autodesk: <https://knowledge.autodesk.com/support/revit-products/learn-explore/caas/>
- CloudHelp/cloudhelp/2021/ENU/Revit-Analyze/files/GUID-925CBF1E-2B91-41A7-8CA8-C87F69F7BBC1.htm.html
- [52] Solar Power Farm. (2021). Retrieved from <https://www.solarpowerfarm.com/cost-of-solar-panels-per-square-meter/>
- [53] SUNMetrix. (2021). Cost of Solar Panels. Retrieved from SUNMetrix: <https://sunmetrix.com/cost-of-solar-panels/#solar1>
- [54] J. Svarc, Clean Energy Reviews Retrieved from <https://www.cleanenergyreviews.info/blog/most-efficient-solar-panels>, 2021.
- [55] C. Sydora, E. Stroulia, Rule-based compliance checking and generative design for building interiors using BIM, *Automation* 120 (2020) 103368, <https://doi.org/10.1016/j.autcon.2020.103368>.
- [56] The eco experts, Solar panels Retrieved from The eco experts: <https://www.theecoexperts.co.uk/solar-panels/how-much-electricity>, 2021.
- [57] Verberne, G. van den Donker, M., (2015). BIPV Pricing in The Netherlands: 2014 Price Benchmark Report. <http://resolver.tudelft.nl/uuid:406b6380-de69-432b-98ae-b64c3c6557cd>, Accessed on 23-11-2021.
- [58] R. Wang, An Improved Nondominated Sorting Genetic Algorithm for Multiobjective Problem, *Mathematical Problems Eng.* 2016 (2016) 1–7.
- [59] J.-H. Yoon, J. Song, S.-J. Lee, Practical application of building integrated photovoltaic (BIPV) system using transparent amorphous silicon thin-film PV module, *Sol. Energy* 85 (5) (2011) 723–733.
- [60] J. Zhang, N. Liu, S. Wang, Generative design and performance optimization of residential buildings based on parametric algorithm, *Energy Build.* 244 (2021) 111033, <https://doi.org/10.1016/j.enbuild.2021.111033>.
- [61] C. Peng, Y. Huang, Z. Wu, Building-integrated photovoltaics (BIPV) in architectural design in China, *Energy and Buildings* 43 (12) (2011) 3592–3598.
- [62] C. Catita, P. Redweik, J. Pereira, Extending solar potential analysis in buildings to vertical facades 66 (2014), <https://doi.org/10.1016/j.cageo.2014.01.002>, Computers & Geosciences.